A front-end DC-DC converter for proton exchange membrane fuel cell systems

Smet, B.J.M.

Award date:
2005

TU/e Eindhoven University of Technology
/Section Electromechanics and Power Electronics

Master of Science Thesis

A front-end DC-DC converter

for Proton Exchange Membrane Fuel Cell systems

EPE 2005-01 **B.J.M. Smet**

Coach(es): Ir. M.A.M. Hendrix, Dr. J.L. Duarte

Eindhoven, February 1, 2005

Preface

This report is about my Master of Science project, which I performed at the Pre Development Center of Philips Lighting Electronics.
I would like to thank Andre Vandenput, chairman of the section Electromechanics and Power Electronics, for helping me to find this project.
Also I would like to thank Leo Verhees and Marcel Hendrix for offering me the position at the Pre Development Center.
For their guidance during the project I would like to thank my supervisors Marcel Hendrix and Jorge Duarte.
Special thanks go out to Ludwig Oostvogels, whom I consulted many times for realization of the magnetic components.
All other colleagues from the Pre Development Center I would to thank for their support and the pleasant working atmosphere.

For their support during not only this project, but also during the rest of my studies I am very grateful to my parents, my sister and all other friends and relatives.

Most grateful I am to the person who helped me back on track during less dynamic periods of my studies, always kept supporting me and never lost her faith in me, my girlfriend, Marije van Dijk.

Abstract

This report is about a Master of Science project that was carried out by a student of the Eindhoven University of Technology (TU/e) at the Pre-Development Centre (PDC) of the business group Lighting Electronics of Philips Lighting BV.

During this project a 2 kW front-end DC-DC converter for Proton Exchange Membrane Fuel Cells (PEMFC) has been designed. The goal of the project is to design a DC-DC converter that can replace the DC-DC converter of the EVO-2000 so the existing DC-AC converter can be reused to obtain an inverter for fuel cell application. The challenge for this design is the very low input voltage of 20 V that leads to an input current of 100 A.

Based on a former Philips report [4] the choice was made to use a four way interleaved boost converter. In this report first a normal boost converter is described. Based on the disadvantages improvements are suggested and so one becomes the suggested topology for the DC-DC converter at the end of chapter 2.

After that, the chosen topology is further described and the influences of parasitic components and component tolerances are investigated. This leads to the conclusion that a control circuit for the duty cycles is necessary to distribute the current equally over the branches.

Based on the equations that describe the circuit, the component values are calculated in chapter 4 and the standard components are chosen and magnetic components are designed. At the end of chapter 4 one can find photos of the realised breadboard of the four way interleaved DC-DC converter.

In chapter 5 the testing of the converter is described. First the measured results are compared to circuit simulations and one concludes that the converter operates as expected. After that one tried to measure the efficiency of the converter, but this is very hard for a converter with such a large input current. From the measurements one concludes that the losses are mainly caused by the leakage inductance of the step-up transformers and that the second largest cause for losses are the parasitic resistances of the magnetic components and the MOSFETs.

Then finally in chapter 6 one concludes that the chosen topology works the way one expected, but that a control circuit has to be designed to equally distribute the currents over the branches. As a follow up of this project one suggests to build a new breadboard where more attention is paid to the connection of the magnetic components and to investigate some ways to decrease the losses caused by the leakage induction of the step-up transformers.

Table of contents

Introduction

This report is about a Master of Science project that was carried out by a student of the Eindhoven University of Technology (TU/e) at the Pre-Development Centre (PDC) of the business group Lighting Electronics of Philips Lighting BV.

At PDC a 2 kW DC-AC converter, the EVO-2000, has been developed to connect solar panels to the grid for small-scale environment friendly energy generation at home. This converter consists of three stages. The first stage is a front-end DC-DC converter that amplifies the input voltage from 75 V to 400V. The second stage is also a DC-DC converter that isolates the solar panel from the grid for safety; it doesn't amplify or attenuate the voltage. And the third and final stage is a DC-AC converter that injects current in the grid.

The goal of this project is to design a new front-end DC-DC converter for fuel cell systems that replaces the former front-end DC-DC converter in such a way that the DC-AC converter of the solar project can be reused and that the effort of designing a new DC-AC converter can be spared.

A fuel cell system is a new source of energy. Simply said, hydrogen is burned and the products of this reaction are water and electricity. Fuel cells are under investigation at the TU/e [3].
There are many types of fuel cell systems. The system used during this project is a Proton Exchange Membrane Fuel Cell (PEMFC).
From an electrical point of view fuel cells are quite similar to solar panels; they both provide a direct voltage. However, fuel cells provide a lower voltage than solar panels and to generate the same input power for the converter the current will be much bigger.

The higher input current can be divided over several boost converters that are connected in parallel. This will prevent the need for exotic components for very high currents. By interleaving the converters, that is controlling them one by one, shifted in time, the ripple currents in the converters will, partially, compensate and the very high input current is nearly ripple-less. This nearly ripple-less current reduces the size of the input filter that is needed to draw a ripple-less current from the fuel cell.
The manufacturer doesn't allow a high frequency current ripple through the fuel cell.

In a former traineeship [5] the isolation stage was already altered for a lower input voltage. The DC-DC amplification of the front-end boost converter would be very high for a three-stage converter where the isolation stage doesn't amplify the voltage. A boost converter with a very high amplification is hard to realise and has a low efficiency. In the traineeship the isolation stage was altered into an isolation stage with amplification of the input voltage. During this project it turned out to be beneficial to integrate the interleaved boost converter and the isolation transformer into one converter.

The result of this project is a front-end DC-DC converter with build in isolation function that makes it possible to connect a fuel cell to the existing DC-AC converter of the EVO-2000.

The report's structure is as follows; first the reader can find the assignment for the project in chapter 1. Then in chapter 2 one can follow the steps that lead to the final design. In chapter 3 the final design is further investigated and the realization of the converter is described in chapter 4. In chapter 5 measurements on the breadboard are compared with simulations and predictions. Finally chapter 6 contains the conclusions that can be made after this project and some recommendations to improve the converter.

1 Assignment

The assignment was to realise a four way interleaved boost converter for a 2 kW fuel cell system. The power should be equally distributed over all four branches.
One should be able to connect the existing DC-AC converter of the EVO-2000 platform to the new DC-DC converter or to the series connection of the new DC-DC converter and the altered isolation stage [5].

This is a very free assignment and during the project some extra demands were made on the converter and the operation of it.

The converter will only be operated at full load. At partial load the output voltage is considerably higher. This has influence on the duty cycle and on the input current ripple.

The input current ripple is limited to 5 %. The fuel cell manufacturer doesn't allow a high frequency ripple through the fuel cell and limiting the input current ripple of the converter reduces the size of the input filter to connect the DC-DC converter to the fuel cell.

The switching frequency is 100 kHz. In the end, one will evaluate if this is a correct choice. The 100 kHz was chosen because this is comparable with the altered isolation stage. However in the altered isolation stage there is no hard switching and there are no switching losses.

2 DC-DC converters

In this chapter, different DC-DC converters will be compared. This was also done during a former Master of Science project [2]. In this report the emphasis will be on the application for fuel cell systems, where there is a very high input current and the demand for a nearly ripple-less input current. First a simple boost converter is described; this converter has several disadvantages for fuel cell applications. Step-by-step the converter will be altered until finally a suitable converter design for fuel cell applications is reached. The final design with the input transformers and the step-up transformers will be further examined in the next chapter and eventually realised and tested.

2.1 Specifications of the DC-DC converter

The input voltage of the converter is the output voltage of a fuel cell at full output power. The voltage characteristic of the fuel cell can be found in [3]. The input voltage of the converter is specified to be 20 V.

The converter is designed for an input power of 2 kW, the input current is then 100 A.

The output voltage of the DC-DC converter is the input voltage of the altered isolation stage of EVO-2000 [5], which is 100 V. The amplification of the DC-DC converter is therefore 5.
The altered isolation stage amplifies the voltage to 400 V, the input voltage of the EVO-2000 inverter.

In [4] the use of an interleaved boost converter is proposed. The duty cycle of a boost converter with an amplification of 5 is 0.8, which will be explained later. In the following paragraphs we will use the fact that the duty cycle is larger than 0.75. Because the duty cycle is higher than 0.75 there are only two states for the circuit; all switches are closed or only one switch is opened.

2.2 A single boost converter

Alternating voltages can easily be amplified by using a transformer. A transformer doesn't amplify direct voltages and a different solution has to be found to amplify the voltage.
One of the solutions is shown in figure 1, it is called a boost converter.
A single boost converter is described in almost every book about power electronics, for example [1].

When the output capacitance C_{out} is large enough one can consider the output voltage to be constant. When the switch S1 is closed there will be a voltage V_{in} over the boost inductor and the current through the inductor will rise. When the switch S1 is opened the current through the inductor can't stop flowing and will flow through the diode D1. The voltage over the boost inductor is now $V_{in} - V_{out}$. When the output voltage is higher than the input voltage the inductor current will now decrease. Now there are two possibilities; the inductor current can become zero before the switch is turned on again or the switch can be turned on before the inductor current reaches zero. The first possibility is called discontinuous conduction mode (DCM) and the second is called continuous conduction mode (CCM). In DCM the peak inductor current is equal to or bigger than twice the mean inductor current. For applications with large mean inductor currents this is not wanted and therefore this mode isn't considered in this report. In CCM the switch turns on before the current through the inductor reaches zero and a new period starts.

Now consider the current through the boost inductor.

The switch S1 is closed during dT and the diode is conducting during (1-d)T. The voltage over the inductor will then be V_{in} during dT and $V_{in} - V_{out}$ during (1-d)T.

For the current through the inductor one can write:

$$\Delta I = \frac{U}{L}\Delta T \tag{1}$$

In steady state the current through the inductor at the end of a period will be equal to the current at the beginning of the period. This leads to the following equation:

$$\frac{V_{in}}{L_{boost}}dT = -\frac{V_{in} - V_{out}}{L_{boost}}(1-d)T \tag{2}$$

Solving equation (2) leads to the following expression for the output voltage:

$$V_{out} = \frac{1}{1-d}V_{in} \tag{3}$$

Because 0<d<1 the output voltage is higher than the input voltage and the assumption before was right.

In figure 2 one can see the relevant component voltages and currents during a complete period in CCM.

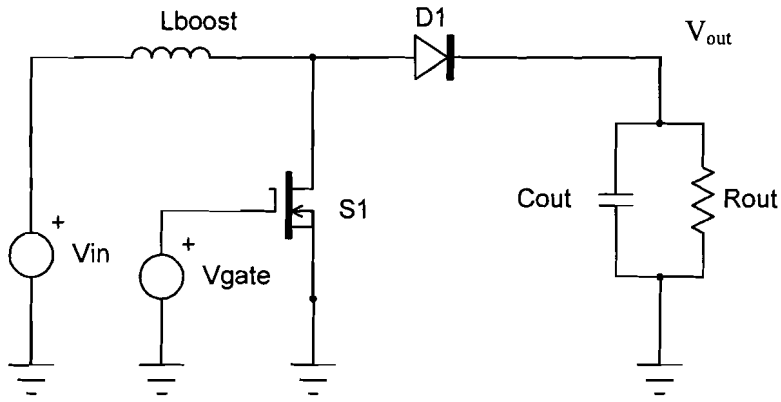

Figure 1: A single boost converter.

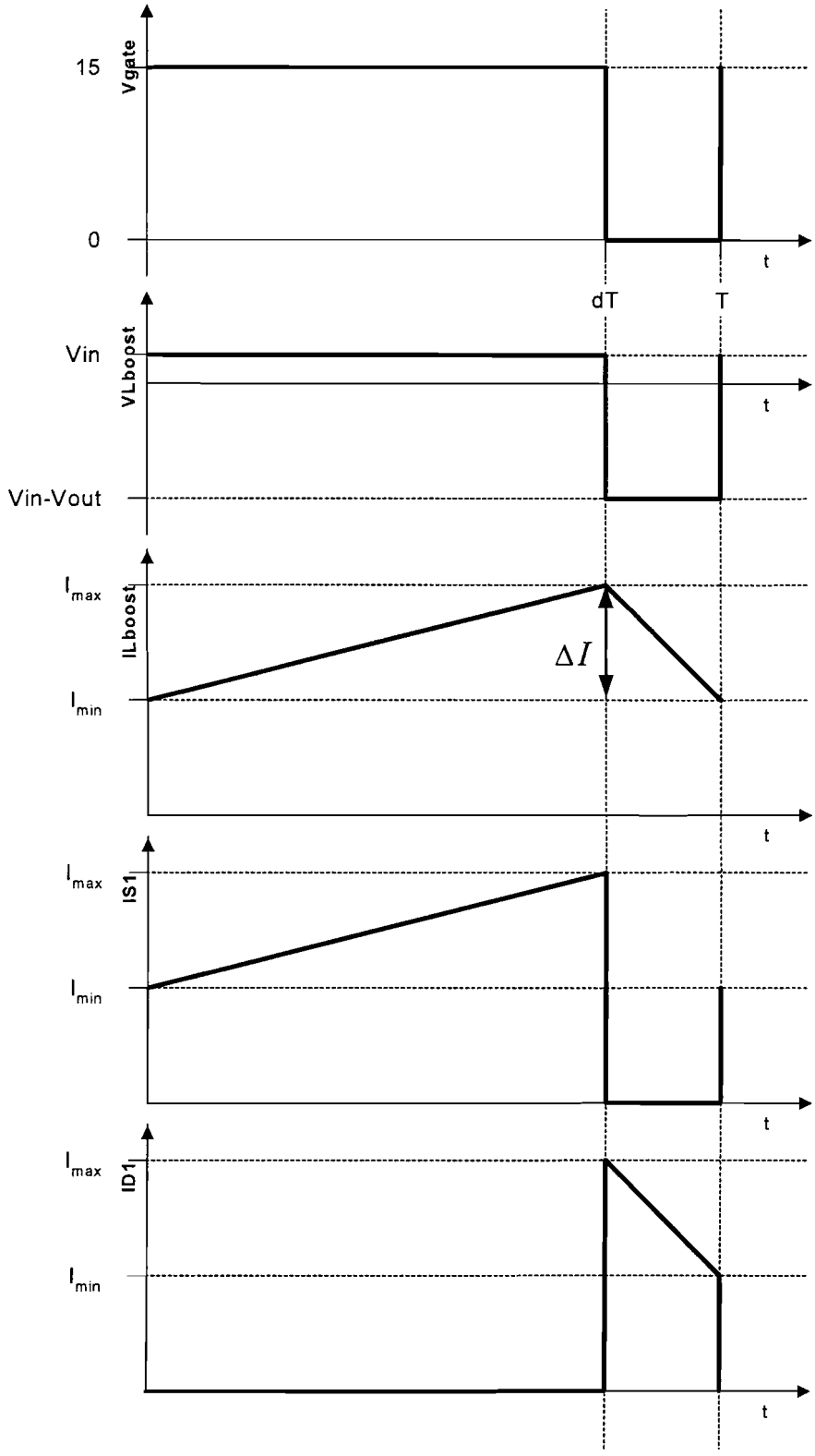

Figure 2: Relevant component voltages and currents during a complete period in CCM.

2.3 Interleaved boost converter

In the boost converter in the preceding paragraph the peak inductor current is still higher than the mean input current, which is very large for the wanted converter. Also the input ripple can only be reduced by increasing the boost inductance. The high peak current and the large inductance lead to a large geometrical constant (see [9]) and a bulky boost inductor.

To reduce the peak current through an inductor, four boost converters can be placed in parallel. By closing the switches not at the same time, but shifted in time one can also reduce the input current ripple.

The paralleling of the converters together with the time-shifted control of the switches is called interleaving. The principle of interleaving and the effect on the input current ripple is well described in literature [6].

The circuit diagram of the four way interleaved boost converter is shown in figure 3. The relevant voltage and current waveforms can be seen in figure 4.

The current ripple in one branch is still given by:

$$\Delta I_{branch} = \frac{V_{in}}{L_{boost}} dT \tag{4}$$

When the phase shift between the branches is T/4 the input current ripple will reach a minimum which is given by:

$$\Delta I_{in} = \frac{4V_{in}}{L_{boost}}(d - 3/4)T = \frac{V_{in}}{L_{boost}}(4d - 3)T = (4 - 3/d)\Delta I_{branch} \tag{5}$$

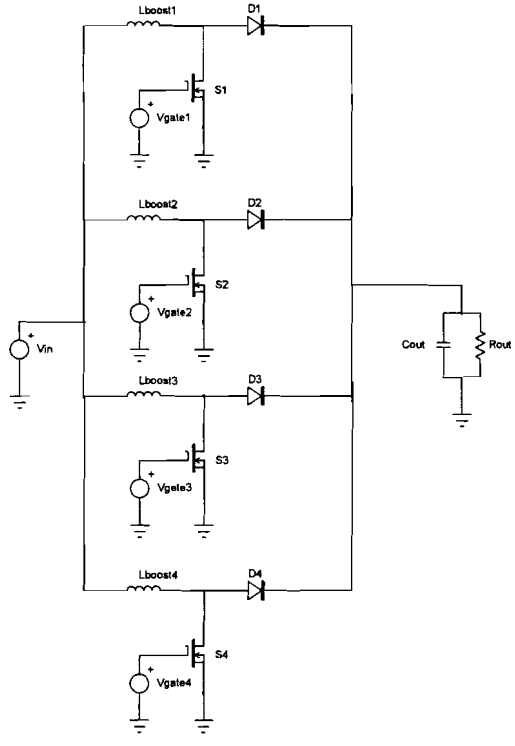

Figure 3: Four way interleaved boost converter.

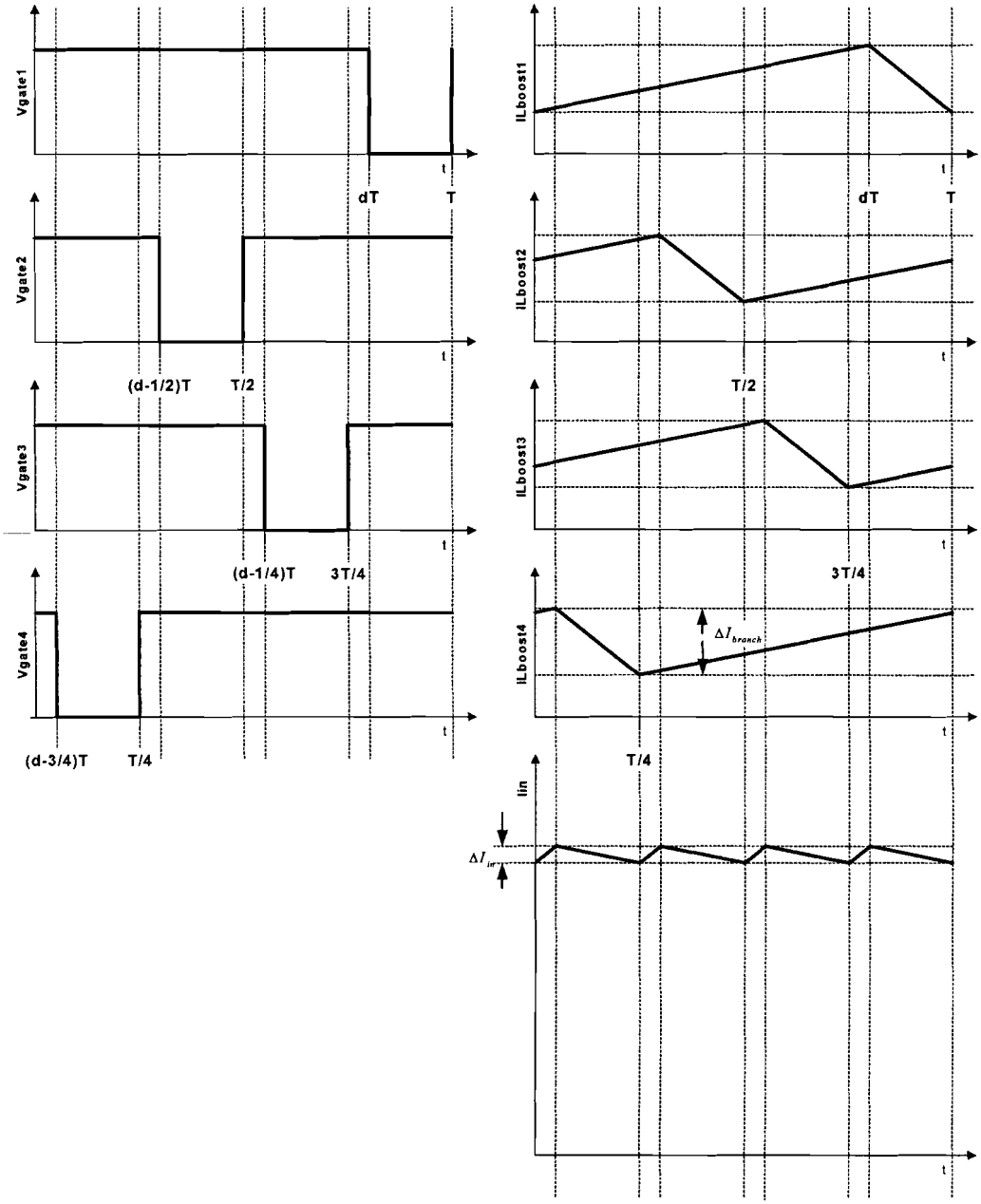

Figure 4: Waveforms in the four way interleaved boost circuit during one complete period with CCM.

2.4 Interleaved boost converter with input transformers

In the preceding paragraph four boost converters were placed in parallel and controlled shifted in time so the input current ripple is strongly attenuated. The nearly ripple-less input current is, however, the sum of four inductor currents that can each still contain a large ripple. The ripple on the branch currents causes core losses in the boost inductor and also enlarges the peak inductor current. The higher peak current asks for a larger boost inductor volume.

The ripple current in the branches can be reduced by using transformers with a turns ratio of minus 1 on the input of the circuit. Such a transformer is shown in figure 5.
The operation of these transformers is well described in literature [7],[8].

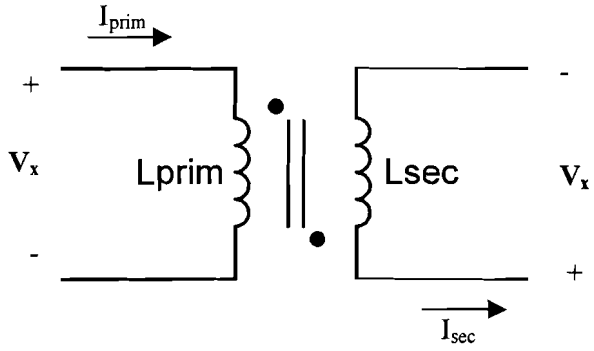

Figure 5: Counter coupled transformer on the input of the circuit.

In an ideal transformer the current I_{prim} will be equal to the current I_{sec}.
The connection of the input transformers can be seen in figure 6. The first transformer will then divide the current in two and the two following transformers make sure that the boost inductor current is one quarter of the input current.
The ripple in the input current is equal to the ripple in the interleaved converter from the previous paragraph, but the ripple in one branch is only one quarter of the ripple of the input current.

Another problem one encounters when interleaving boost converters is that the converters act as voltage sources. Small differences in the converters lead to output voltage differences and the input current isn't equally distributed over the branches. The input transformers have been described in literature as components that distribute the input current equally over the branches. In the next chapter the distribution of the current over the branches as a function of parasitic components and component tolerances will be investigated.

The circuit of the converter can be seen in figure 6 and the corresponding wave shapes can be seen in figure 7.

When the duty cycle of the boost converters is higher than 0.75 and the phase shift between the branches is T/4 there are only 5 different states for the circuit.

These are:
S0: All the switches are closed
S1: Switch 1 is open and the other three are closed
S2: Switch 2 is open and the other three are closed
S3: Switch 3 is open and the other three are closed
S4: Switch 4 is open and the other three are closed

During each state the inductor currents and therefore all current derivatives are equal. For an inductor one can write: $\frac{di}{dt} = \frac{V}{L}$.

When one assumes that all inductances are equal this leads to the following equations:

S0:

$$\left.\begin{aligned} V_{Lboost1} &= V_{in} - V_x - V_y \\ V_{Lboost2} &= V_{in} - V_x + V_y \end{aligned}\right\} V_{Lboost1} = V_{Lboost2} \Rightarrow V_y = 0$$

$$\left.\begin{aligned} V_{Lboost3} &= V_{in} + V_x - V_z \\ V_{Lboost4} &= V_{in} + V_x + V_z \end{aligned}\right\} V_{Lboost3} = V_{Lboost4} \Rightarrow V_z = 0$$

$$\left.\begin{aligned} V_{Lboost1} = V_{Lboost2} \Rightarrow V_y = 0 \\ V_{Lboost3} = V_{Lboost4} \Rightarrow V_z = 0 \end{aligned}\right\} V_{Lboost1} = V_{Lboost3} \Rightarrow V_x = 0$$

S1:

$$\left.\begin{aligned} V_{Lboost1} &= V_{in} - V_x - V_y - V_{out} \\ V_{Lboost2} &= V_{in} - V_x + V_y \end{aligned}\right\} V_{Lboost1} = V_{Lboost2} \Rightarrow V_y = -\frac{V_{out}}{2}$$

$$\left.\begin{aligned} V_{Lboost3} &= V_{in} + V_x - V_z \\ V_{Lboost4} &= V_{in} + V_x + V_z \end{aligned}\right\} V_{Lboost3} = V_{Lboost4} \Rightarrow V_z = 0$$

$$\left.\begin{aligned} V_{Lboost1} = V_{Lboost2} \Rightarrow V_y = -\frac{V_{out}}{2} \\ V_{Lboost3} = V_{Lboost4} \Rightarrow V_z = 0 \end{aligned}\right\} V_{Lboost2} = V_{Lboost3} \Rightarrow V_x = -\frac{V_{out}}{4}$$

S2:

$$\left.\begin{aligned} V_{Lboost1} &= V_{in} - V_x - V_y \\ V_{Lboost2} &= V_{in} - V_x + V_y - V_{out} \end{aligned}\right\} V_{Lboost1} = V_{Lboost2} \Rightarrow V_y = \frac{V_{out}}{2}$$

$$\left.\begin{aligned} V_{Lboost3} &= V_{in} + V_x - V_z \\ V_{Lboost4} &= V_{in} + V_x + V_z \end{aligned}\right\} V_{Lboost3} = V_{Lboost4} \Rightarrow V_z = 0$$

$$\left.\begin{aligned} V_{Lboost1} = V_{Lboost2} \Rightarrow V_y = \frac{V_{out}}{2} \\ V_{Lboost3} = V_{Lboost4} \Rightarrow V_z = 0 \end{aligned}\right\} V_{Lboost1} = V_{Lboost3} \Rightarrow V_x = -\frac{V_{out}}{4}$$

S3:

$$\left.\begin{aligned} V_{Lboost1} &= V_{in} - V_x - V_y \\ V_{Lboost2} &= V_{in} - V_x + V_y \end{aligned}\right\} V_{Lboost1} = V_{Lboost2} \Rightarrow V_y = 0$$

$$\left.\begin{aligned} V_{Lboost3} &= V_{in} + V_x - V_z - V_{out} \\ V_{Lboost4} &= V_{in} + V_x + V_z \end{aligned}\right\} V_{Lboost3} = V_{Lboost4} \Rightarrow V_z = -\frac{V_{out}}{2}$$

$$\left.\begin{aligned} V_{Lboost1} = V_{Lboost2} \Rightarrow V_y = 0 \\ V_{Lboost3} = V_{Lboost4} \Rightarrow V_z = -\frac{V_{out}}{2} \end{aligned}\right\} V_{Lboost1} = V_{Lboost4} \Rightarrow V_x = \frac{V_{out}}{4}$$

S4:

$$\left.\begin{aligned} V_{Lboost1} &= V_{in} - V_x - V_y \\ V_{Lboost2} &= V_{in} - V_x + V_y \end{aligned}\right\} V_{Lboost1} = V_{Lboost2} \Rightarrow V_y = 0$$

$$\left.\begin{aligned} V_{Lboost3} &= V_{in} + V_x - V_z \\ V_{Lboost4} &= V_{in} + V_x + V_z - V_{out} \end{aligned}\right\} V_{Lboost3} = V_{Lboost4} \Rightarrow V_z = \frac{V_{out}}{2}$$

$$\left.\begin{aligned} V_{Lboost1} = V_{Lboost2} \Rightarrow V_y = 0 \\ V_{Lboost3} = V_{Lboost4} \Rightarrow V_z = \frac{V_{out}}{2} \end{aligned}\right\} V_{Lboost1} = V_{Lboost3} \Rightarrow V_x = \frac{V_{out}}{4}$$

Now the voltages V_x, V_y and V_z are known during a cycle of the converter operation, one also knows the voltages over the boost inductors. Since all the voltages are equal only one expression has to be evaluated during a period. When all switches are closed the voltage over an inductor is V_{in} and when one switch is open the voltage over an inductor is $V_{in} - V_{out}/4$.

Substituting these voltages in $\Delta I = \frac{V}{L}\Delta t$ leads to:

$$\Delta I_{branch} = \frac{V_{in}}{L_{boost}}(d - 3/4)T \tag{6}$$

And the input current is the sum of the four inductor currents so:

$$\Delta I_{in} = 4\Delta I_{branch} = \frac{4V_{in}}{L_{boost}}(d - 3/4)T = \frac{V_{in}}{L_{boost}}(4d - 3)T \tag{7}$$

Here one can see that the input current ripple is equal to the situation where the input transformers weren't placed in the circuit and that the reduction of the ripple in one branch caused by the transformers is eq. (4)/ eq. (6), which is: $\frac{4d}{4d-3}$

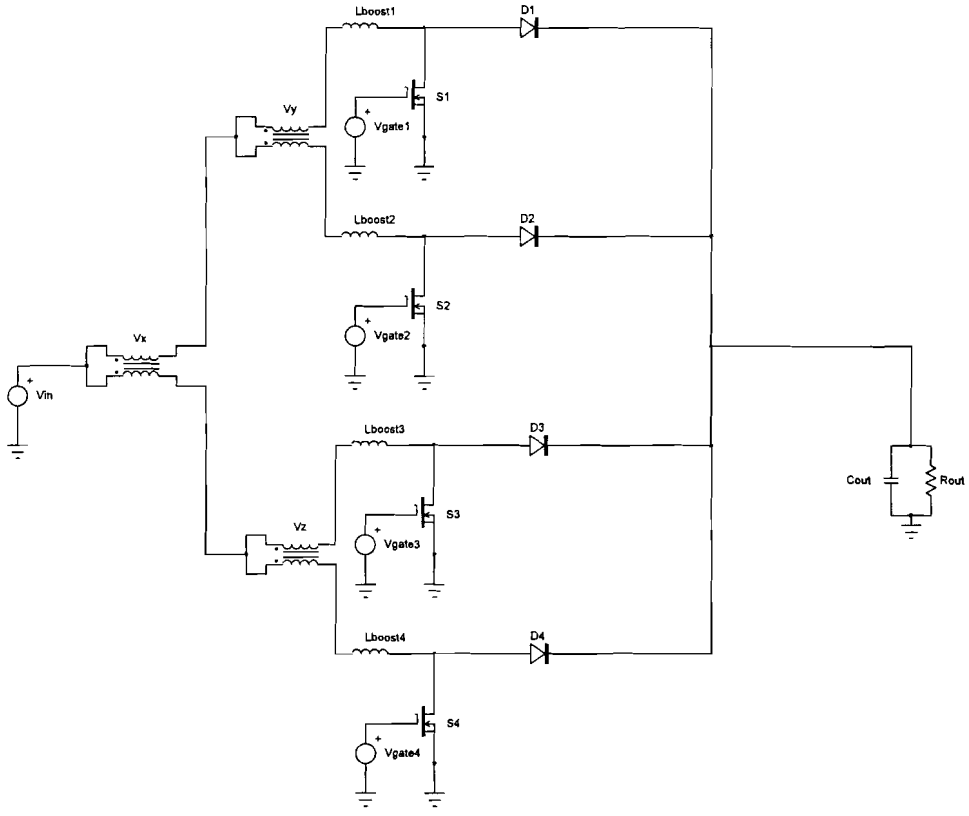

Figure 6: Four way interleaved boost converter with input transformers. The transformers x, y and z have a turns ratio of minus 1.

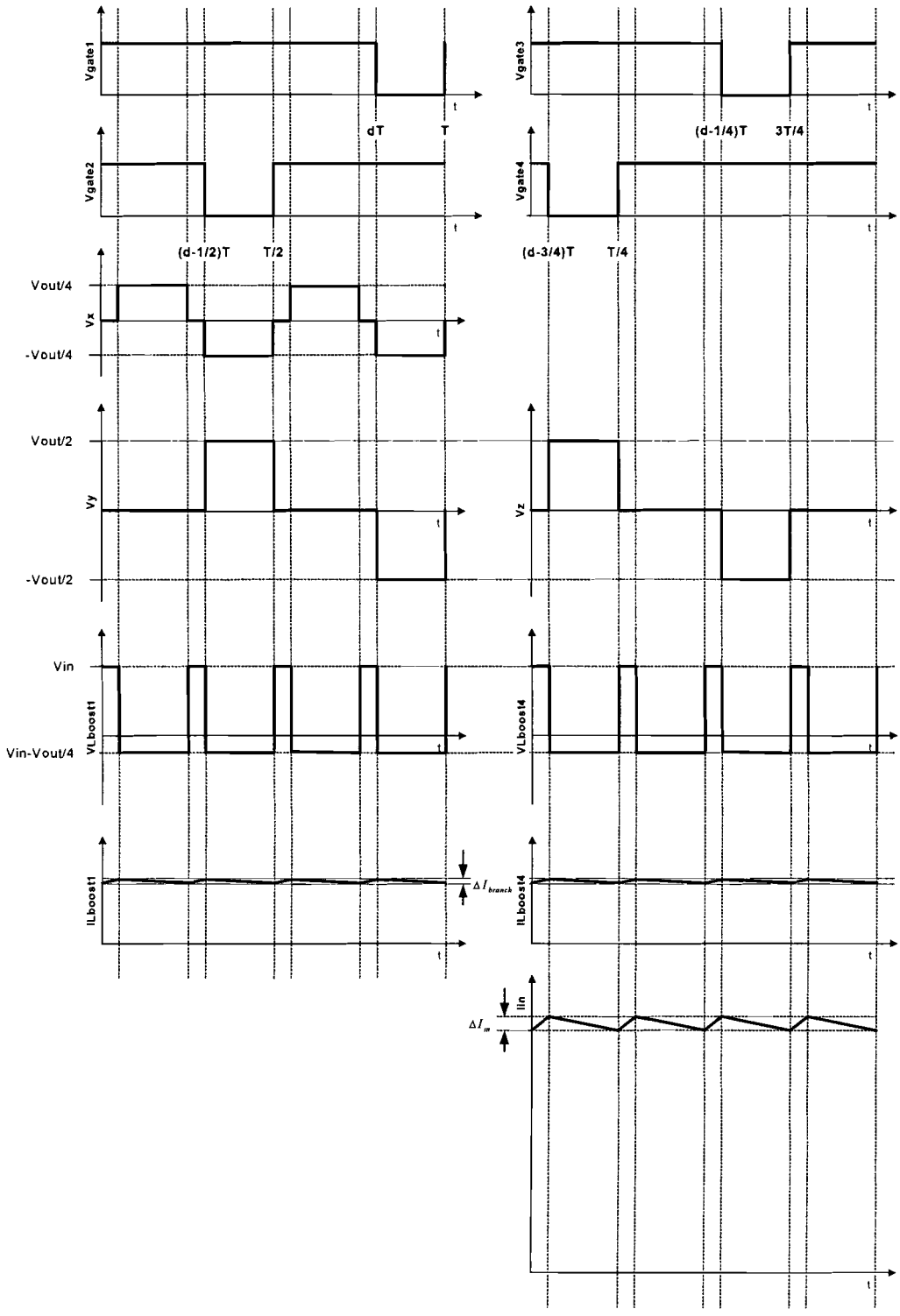

Figure 7: Waveforms of the four way interleaved boost converter with input transformers.

2.5 Interleaved boost converter with input- and step-up transformers

The preceding converter had an input voltage of 20 V and an output voltage of 100 V. The converter will be connected to the isolation stage, which will amplify the voltage to 400 V. The output stage of the DC-DC converter however consists of diodes, which rectify the voltage and the input stage of the isolation stage is a full bridge circuit to produce a square wave voltage that can be transformed. There will be forward conduction and reverse recovery losses in the diodes, which are hard switched and resistive losses in the MOSFETs of the full bridge. Therefore the diodes and the MOSFETs are left out of the circuit; the transformers will be directly connected to the drains of the MOSFETs and the diodes on the secondary side of the transformers function as boost diodes. This is illustrated in figure 8. The current switched by the boost diodes is smaller and therefore the forward conduction losses and the reverse recovery losses will be lower. Moreover the leakage inductance of the transformer is connected in series with the diodes and limits the current drop, which will even further reduce the reverse recovery losses.

Because the converter consists of four branches two transformers are needed to amplify the voltage from 100 V to 400 V. The total converter now amplifies the voltage from 20 V to 400 V and has a build in isolation function. The schematic for the converter is given in figure 9 and the relevant waveforms are shown in figure 10.

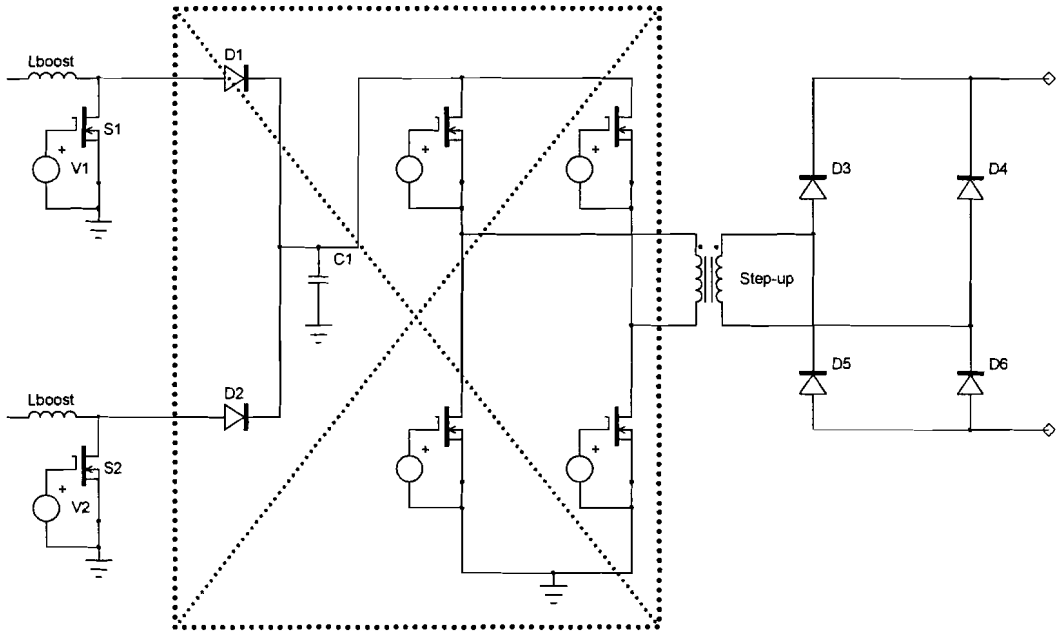

Figure 8: Reduction of number of components by combining boost and isolation stage.

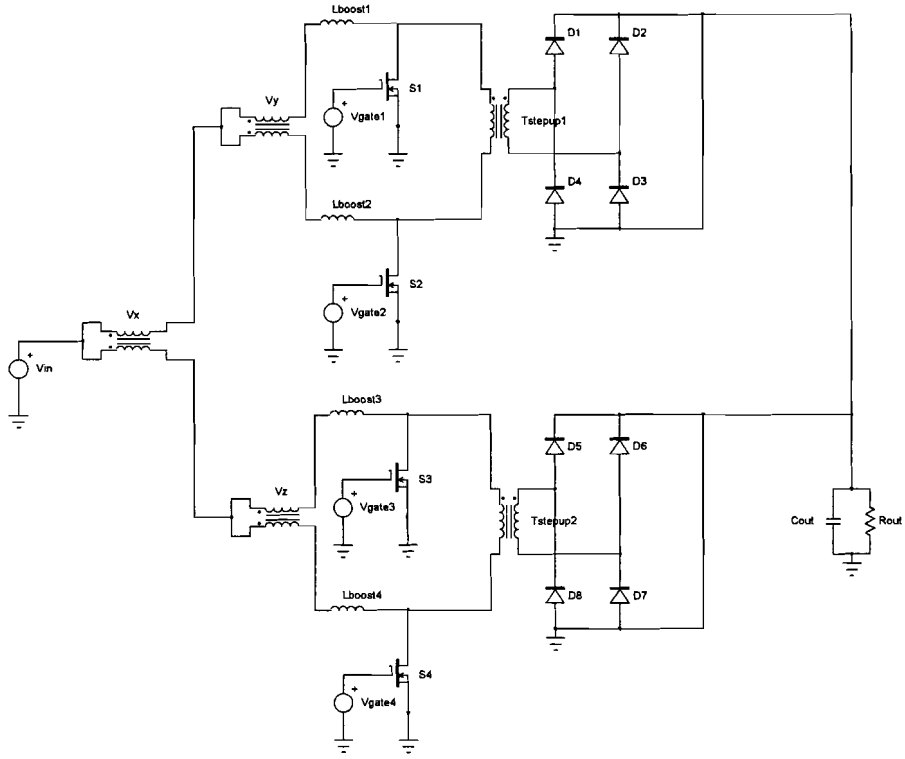

Figure 9: Four way interleaved boost converter with input- and step-up transformers. The transformers x, y and z have a turns ratio of minus 1.

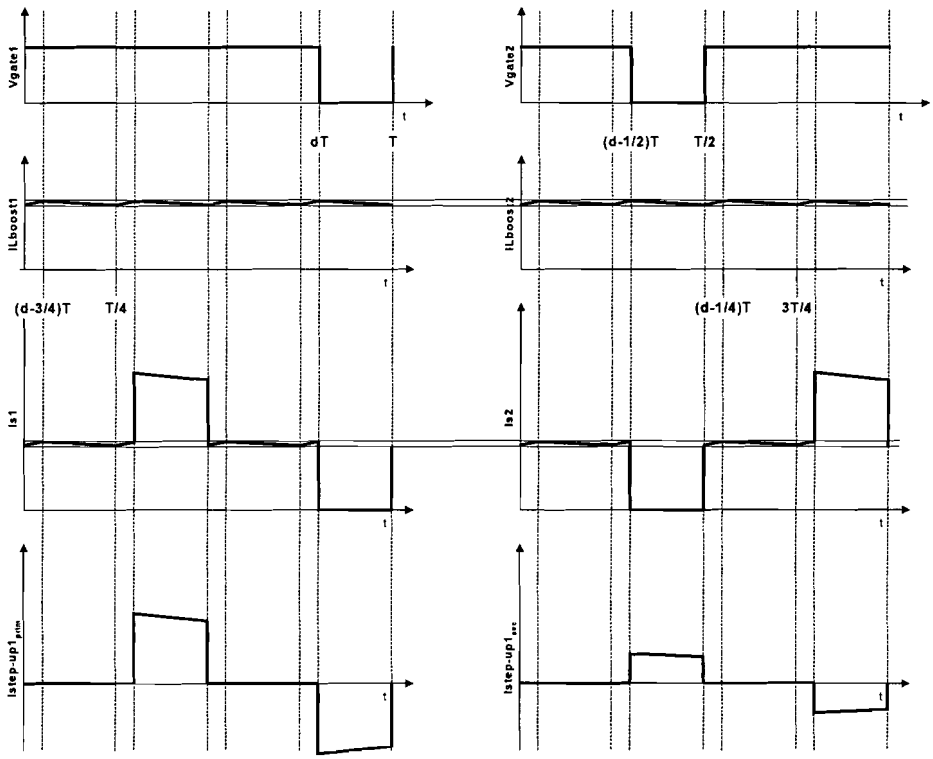

Figure 10: Waveforms of the interleaved converter with input- and step-up transformers.

3 The DC-DC converter for PEMFC systems

In the previous chapter a circuit for the DC-DC converter was suggested. The operation of the circuit with ideal components was described. In this chapter the operation will be described when the circuit contains non-ideal components. First the operation will be described when the non-ideal components are equal in the different branches. After that the distribution of current and power over the branches will be discussed when there is a difference between the components in the branches.

3.1 Changes in the converter characteristics caused by non-ideal components

In figure 11 the circuit is given with several non-ideal components. The input transformers have a turns ratio of minus 1 as was mentioned in the previous chapter. The transformers, MOSFETs and inductors have non-zero resistances and the transformers have finite magnetizing inductances and leakage inductances.
These parasitic components have consequences for the waveforms in the converter.

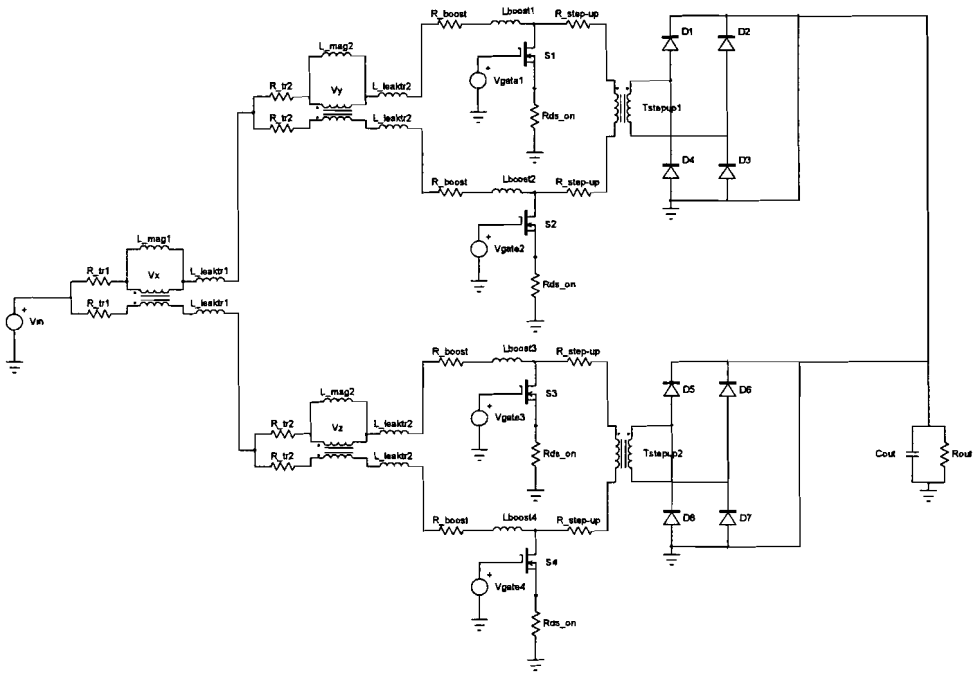

Figure 11: DC-DC converter with several non-ideal components. The transformers x, y and z have a turns ratio of minus 1.

In this paragraph first there will be a derivation of the influence of the magnetizing inductance of the input transformers. Second the circuit will be examined when the components have finite conductance. In paragraph 3.2 there will be an analysis of what happens to the distribution of the current when there are differences in the components in the different branches.

3.1.1 Influence of the magnetizing inductance of the input transformers

In figure 12 one can see the circuit of the PEMFC converter with input transformers with a finite magnetizing inductance.

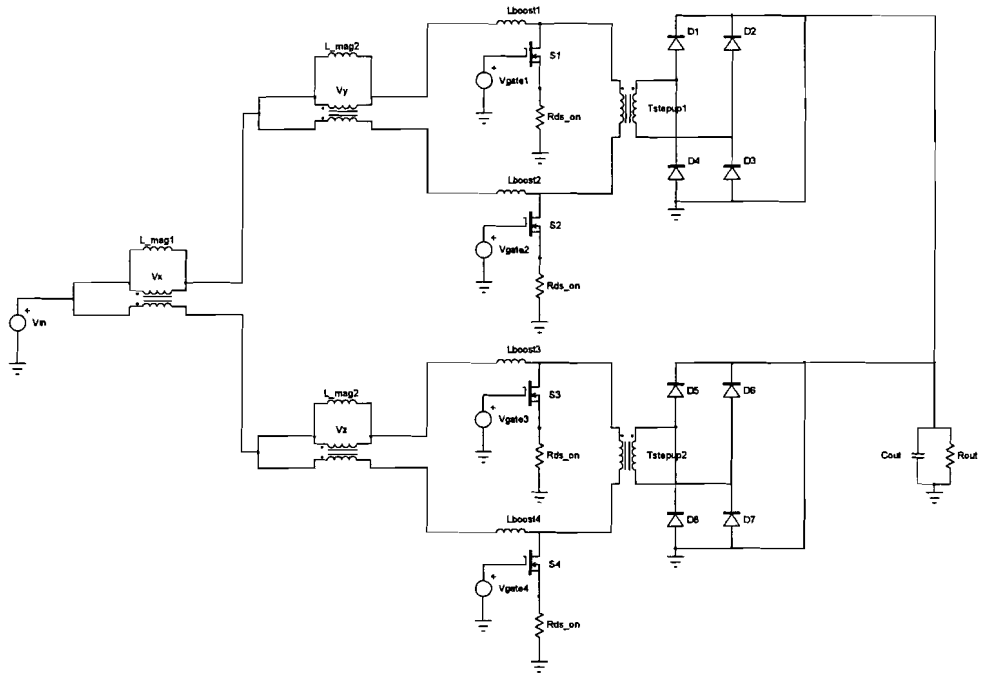

Figure 12: Circuit with finite magnetizing inductance in the input transformers. The transformers x, y and z have a turns ratio of minus 1.

When the magnetizing currents of the input transformers aren't neglected one can write the following for the currents in the branches:

$$i_1 = i_{Lboost1} = i_{Lboost2} + i_{L\_mag2} = i_{Lboost4} + i_{L\_mag1} + i_{L\_mag2}$$

$$i_2 = i_{Lboost2} = i_{Lboost4} + i_{L\_mag1}$$

$$i_3 = i_{Lboost3} = i_{Lboost4} + i_{L\_mag2}$$

$$i_4 = i_{Lboost4}$$

Taking the derivative leads to:

$$\frac{d}{dt}i_1 = \frac{d}{dt}i_{Lboost1} = \frac{d}{dt}i_{Lboost2} + \frac{d}{dt}i_{L\_mag2} = \frac{d}{dt}i_{Lboost4} + \frac{d}{dt}i_{L\_mag1} + \frac{d}{dt}i_{L\_mag2}$$

$$\frac{d}{dt}i_2 = \frac{d}{dt}i_{Lboost2} = \frac{d}{dt}i_{Lboost4} + \frac{d}{dt}i_{L\_mag1}$$

$$\frac{d}{dt}i_3 = \frac{d}{dt}i_{Lboost3} = \frac{d}{dt}i_{Lboost4} + \frac{d}{dt}i_{L\_mag2}$$

$$\frac{d}{dt}i_4 = \frac{d}{dt}i_{Lboost4}$$

When one assumes that all boost inductances are L_{boost}, the magnetizing inductance of the first input transformer is L_{mag1} and the magnetizing inductance of the second input transformer is L_{mag2}, one can write:

$$L_{boost}\frac{d}{dt}i_1 = L_{boost}\frac{d}{dt}i_{Lboost2} + \frac{L_{boost}}{L_{mag2}}L_{mag2}\frac{d}{dt}i_{L\_mag2}$$

$$L_{boost}\frac{d}{dt}i_2 = L_{boost}\frac{d}{dt}i_{Lboost4} + \frac{L_{boost}}{L_{mag1}}L_{mag1}\frac{d}{dt}i_{L\_mag1}$$

$$L_{boost}\frac{d}{dt}i_3 = L_{boost}\frac{d}{dt}i_{Lboost4} + \frac{L_{boost}}{L_{mag2}}L_{mag2}\frac{d}{dt}i_{L\_mag2}$$

$$L_{boost}\frac{d}{dt}i_4 = L_{boost}\frac{d}{dt}i_{Lboost4}$$

When one replaces L_{boost}/L_{mag1} with σ_1 and L_{boost}/L_{mag2} with σ_2 this becomes:

$$V_{L\_boost1} = V_{L\_boost2} + \sigma_2 V_y = V_{L\_boost4} + \sigma_1 V_x + \sigma_2 V_y$$
$$V_{L\_boost2} = V_{L\_boost4} + \sigma_1 V_x$$
$$V_{L\_boost3} = V_{L\_boost4} + \sigma_2 V_y$$
$$V_{L\_boost4} = V_{L\_boost4}$$

Because the duty cycle of the switches is higher than 0.75 and the phase shift between the branches is T/4 there are only five different states for the circuit:
S0: All switches are closed.
S1: Only switch 1 is open, the rest are closed.
S2: Only switch 2 is open, the rest are closed.
S3: Only switch 3 is open, the rest are closed.
S4: Only switch 4 is open, the rest are closed.

During S0:

$$V_{L\_boost1} = V_{L\_boost2} + \sigma_2 V_y = V_{L\_boost4} + \sigma_1 V_x + \sigma_2 V_y = V_{in} - V_x - V_y$$
$$V_{L\_boost2} = V_{L\_boost4} + \sigma_1 V_x = V_{in} - V_x + V_y$$
$$V_{L\_boost3} = V_{L\_boost4} + \sigma_2 V_z = V_{in} + V_x - V_z$$
$$V_{L\_boost4} = V_{L\_boost4} = V_{in} + V_x + V_z$$

$$V_{L\_boost3} - V_{L\_boost4} = \sigma_2 V_z = -2V_z \Rightarrow V_z = 0$$
$$V_{L\_boost1} - V_{L\_boost2} = \sigma_2 V_y = -2V_y \Rightarrow V_y = 0$$
$$V_{L\_boost2} - V_{L\_boost4} = \sigma_1 V_x = -2V_x \Rightarrow V_x = 0$$

During S1:

$$V_{L\_boost1} = V_{L\_boost2} + \sigma_2 V_y = V_{L\_boost4} + \sigma_1 V_x + \sigma_2 V_y = V_{in} - V_x - V_y - V_{out}$$
$$V_{L\_boost2} = V_{L\_boost4} + \sigma_1 V_x = V_{in} - V_x + V_y$$
$$V_{L\_boost3} = V_{L\_boost4} + \sigma_2 V_z = V_{in} + V_x - V_z$$
$$V_{L\_boost4} = V_{L\_boost4} = V_{in} + V_x + V_z$$

$$V_{L\_boost3} - V_{L\_boost4} = \sigma_2 V_z = -2V_z \Rightarrow V_z = 0$$

$$V_{L\_boost1} - V_{L\_boost2} = \sigma_2 V_y = -2V_y - V_{out} \Rightarrow V_y = \frac{-1}{2+\sigma_2} V_{out}$$

$$V_{L\_boost1} - V_{L\_boost4} = \sigma_1 V_x + \sigma_2 V_y = -2V_x - V_y - V_{out}$$
$$= \sigma_1 V_x - \frac{\sigma_2}{2+\sigma_2} V_{out} = -2V_x + \frac{1}{2+\sigma_2} V_{out} - V_{out}$$
$$\Rightarrow V_x = \frac{-1}{(2+\sigma_2)(2+\sigma_1)} V_{out}$$

During S2:

$$V_{L\_boost1} = V_{L\_boost2} + \sigma_2 V_y = V_{L\_boost4} + \sigma_1 V_x + \sigma_2 V_y = V_{in} - V_x - V_y$$
$$V_{L\_boost2} = V_{L\_boost4} + \sigma_1 V_x = V_{in} - V_x + V_y - V_{out}$$
$$V_{L\_boost3} = V_{L\_boost4} + \sigma_2 V_z = V_{in} + V_x - V_z$$
$$V_{L\_boost4} = V_{L\_boost4} = V_{in} + V_x + V_z$$

$$V_{L\_boost3} - V_{L\_boost4} = \sigma_2 V_z = -2V_z \Rightarrow V_z = 0$$

$$V_{L\_boost1} - V_{L\_boost2} = \sigma_2 V_y = -2V_y + V_{out} \Rightarrow V_y = \frac{1}{2+\sigma_2} V_{out}$$

$$V_{L\_boost2} - V_{L\_boost4} = \sigma_1 V_x = -2V_x + V_y - V_{out}$$
$$= \sigma_1 V_x = -2V_x + \frac{1}{2+\sigma_2} V_{out} - V_{out}$$
$$\Rightarrow V_x = \frac{-(1+\sigma_2)}{(2+\sigma_2)(2+\sigma_1)} V_{out}$$

During S3:

$$V_{L\_boost1} = V_{L\_boost2} + \sigma_2 V_y \quad = V_{L\_boost4} + \sigma_1 V_x + \sigma_2 V_y \quad = V_{in} - V_x - V_y$$
$$V_{L\_boost2} = V_{L\_boost4} + \sigma_1 V_x \quad = \quad = V_{in} - V_x + V_y$$
$$V_{L\_boost3} = V_{L\_boost4} + \sigma_2 V_z \quad = \quad = V_{in} + V_x - V_z - V_{out}$$
$$V_{L\_boost4} = V_{L\_boost4} \quad = \quad = V_{in} + V_x + V_z$$

$$V_{L\_boost3} - V_{L\_boost4} = \sigma_2 V_z = -2V_z - V_{out} \Rightarrow V_z = \frac{-1}{2+\sigma_2} V_{out}$$
$$V_{L\_boost1} - V_{L\_boost2} = \sigma_2 V_y = -2V_y \Rightarrow V_y = 0$$
$$V_{L\_boost1} - V_{L\_boost4} = \sigma_1 V_x = -2V_x - V_z$$
$$= \sigma_1 V_x = -2V_x + \frac{1}{2+\sigma_2} V_{out}$$
$$\Rightarrow V_x = \frac{1}{(2+\sigma_2)(2+\sigma_1)} V_{out}$$

During S4:

$$V_{L\_boost1} = V_{L\_boost2} + \sigma_2 V_y \quad = V_{L\_boost4} + \sigma_1 V_x + \sigma_2 V_y \quad = V_{in} - V_x - V_y$$
$$V_{L\_boost2} = V_{L\_boost4} + \sigma_1 V_x \quad = \quad = V_{in} - V_x + V_y$$
$$V_{L\_boost3} = V_{L\_boost4} + \sigma_2 V_z \quad = \quad = V_{in} + V_x - V_z$$
$$V_{L\_boost4} = V_{L\_boost4} \quad = \quad = V_{in} + V_x + V_z - V_{out}$$

$$V_{L\_boost3} - V_{L\_boost4} = \sigma_2 V_z = -2V_z + V_{out} \Rightarrow V_z = \frac{1}{(2+\sigma_2)} V_{out}$$
$$V_{L\_boost1} - V_{L\_boost2} = \sigma_2 V_y = -2V_y \Rightarrow V_y = 0$$
$$V_{L\_boost2} - V_{L\_boost4} = \sigma_1 V_x = -2V_x - V_z + V_{out}$$
$$= \sigma_1 V_x = -2V_x - \frac{1}{(2+\sigma_2)} V_{out} + V_{out}$$
$$\Rightarrow V_x = \frac{1+\sigma_2}{(2+\sigma_1)(2+\sigma_2)} V_{out}$$

The voltages over the inductors now look like in figure 13.

Without the magnetizing inductance the fall of the current in a branch during the opening of a switch was equal, independent of which switch was opened. With the magnetizing inductance however the fall will be bigger when the switch in the branch is opened and smaller when the switch in another branch is opened. The rise of the current is still equal every time all switches are closed. Therefore the ripple in the branches will increase. The input current will not change because of the magnetizing inductance. Also the magnetizing inductance doesn't have an effect on the distribution of the current over the branches.

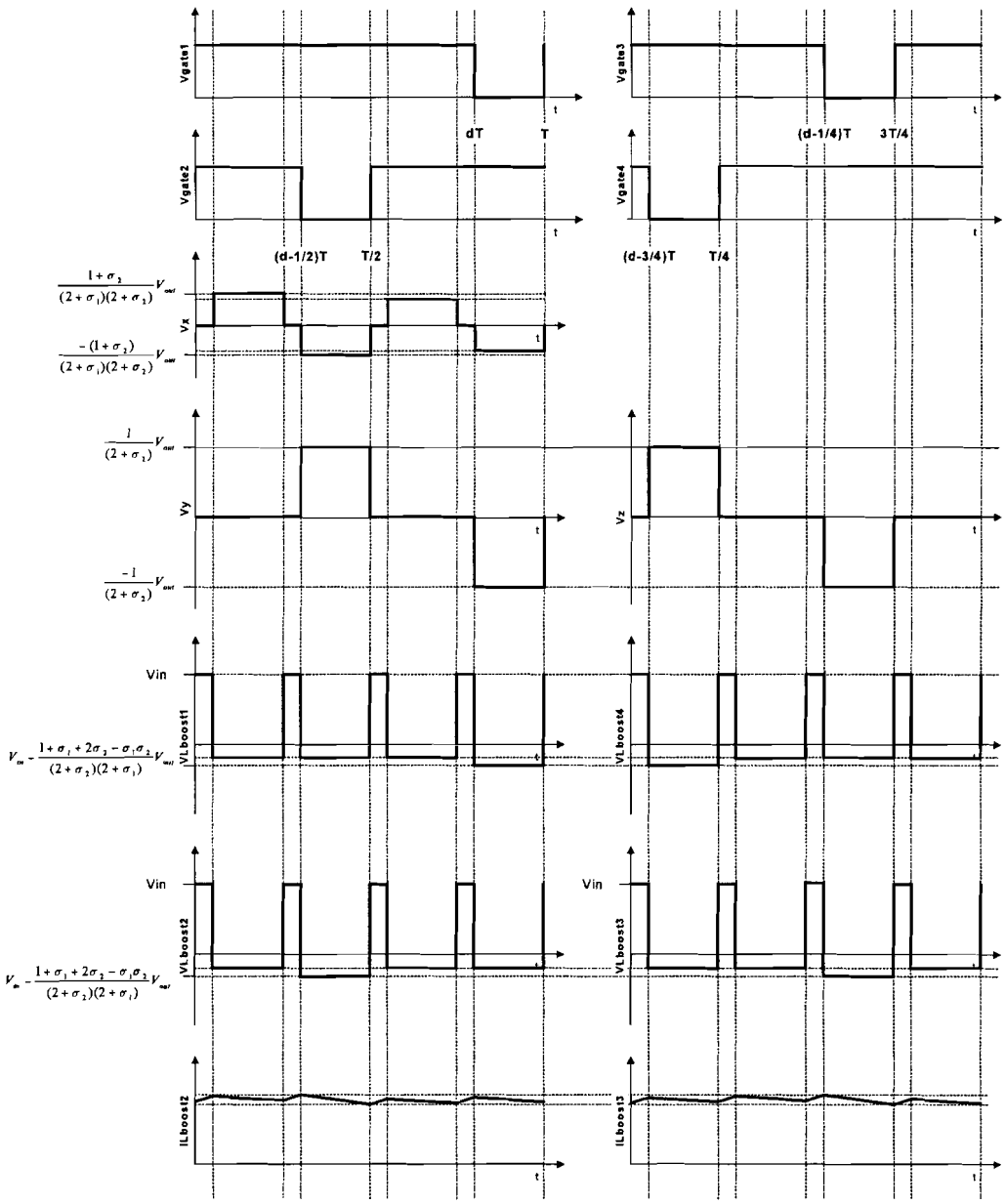

Figure 13: Circuit voltages with finite magnetizing inductance.

3.1.2 Influence of the resistances in the circuit

In figure 14 one can see the PEMFC circuit with non-zero resistances of the boost inductor, the MOSFETs and the step-up transformer. The input transformers have massive wires and only 2 or 3 windings so their resistances are neglected.

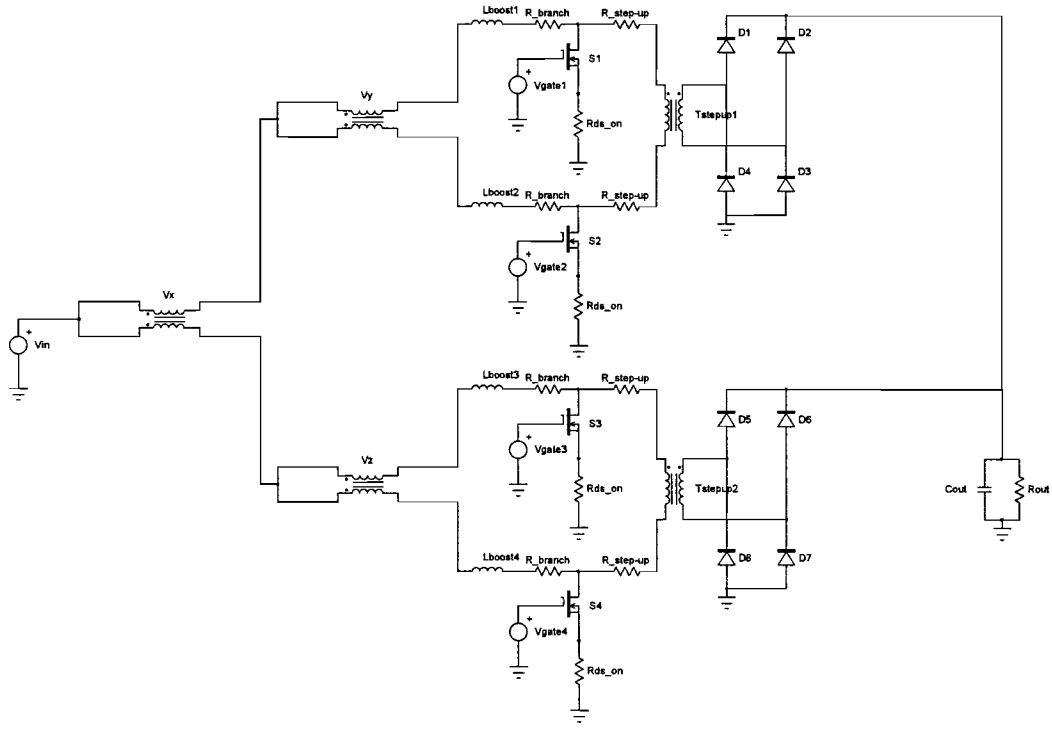

Figure 14: DC-DC converter circuit with non-zero resistances. The transformers x, y and z have a turns ratio of minus 1.

Again the circuit will be described during S0 to S4.

During S0:

$$V_{L\_boost1} = V_{in} - V_x - V_y - (R_{branch} + R_{ds\_on})I_1 \quad (8)$$
$$V_{L\_boost2} = V_{in} - V_x + V_y - (R_{branch} + R_{ds\_on})I_2$$
$$V_{L\_boost3} = V_{in} + V_x - V_z - (R_{branch} + R_{ds\_on})I_3$$
$$V_{L\_boost4} = V_{in} + V_x + V_z - (R_{branch} + R_{ds\_on})I_4$$

The input current is divided into four equal currents with a small ripple so one can assume: $I_1=I_2=I_3=I_4=I_{branch}$. The currents are equal and because the inductances are equal also the voltage should be equal.

$$V_{L\_boost1} - V_{L\_boost2} = -2V_y = 0 \Rightarrow V_y = 0$$
$$V_{L\_boost3} - V_{L\_boost4} = -2V_z = 0 \Rightarrow V_z = 0$$
$$V_{L\_boost1} - V_{L\_boost4} = -2V_x = 0 \Rightarrow V_x = 0$$

By substituting $I_{branch}R_{branch}=V_B$ and $I_{branch}R_{ds\_on}=V_S$, (8) can be rewritten as:

$$V_{L\_boost} = V_{L\_boost1} = V_{L\_boost2} = V_{L\_boost3} = V_{L\_boost4} = V_{in} - (V_B + V_s)$$

Now one can also define $I_{branch}2R_{step\_up}=V_T$. This will be used in the expressions for S1 to S4.

During S1:

$$V_{L\_boost1} = V_{in} - V_x - V_y - V_{out} - V_B - 2V_S - I_{branch}2R_{step\_up}$$
$$= V_{in} - V_x - V_y - V_{out} - V_B - 2V_S - V_T$$
$$V_{L\_boost2} = V_{in} - V_x + V_y - V_B - 2V_S$$
$$V_{L\_boost3} = V_{in} + V_x - V_z - V_B - V_S$$
$$V_{L\_boost4} = V_{in} + V_x + V_z - V_B - V_S$$

$$V_{L\_boost1} - V_{L\_boost2} = -2V_y - V_{out} - V_T = 0 \Rightarrow V_y = \frac{-(V_{out} + V_T)}{2}$$
$$V_{L\_boost3} - V_{L\_boost4} = -2V_z = 0 \Rightarrow V_z = 0$$
$$V_{L\_boost1} - V_{L\_boost4} = -2V_x - V_y - V_{out} - V_s - V_T = 0 \Rightarrow V_x = \frac{-(V_{out} + V_T + 2V_s)}{4}$$

During S2:

$$V_{L\_boost1} = V_{in} - V_x - V_y - V_B - 2V_S$$
$$V_{L\_boost2} = V_{in} - V_x + V_y - V_{out} - V_B - V_T - 2V_S$$
$$V_{L\_boost3} = V_{in} + V_x - V_z - V_B - V_S$$
$$V_{L\_boost4} = V_{in} + V_x + V_z - V_B - V_S$$

$$V_{L\_boost1} - V_{L\_boost2} = -2V_y + V_{out} + V_T = 0 \Rightarrow V_y = \frac{V_{out} + V_T}{2}$$
$$V_{L\_boost3} - V_{L\_boost4} = -2V_z = 0 \Rightarrow V_z = 0$$
$$V_{L\_boost1} - V_{L\_boost4} = -2V_x - V_y - V_s = 0 \Rightarrow V_x = \frac{-(V_{out} + V_T + 2V_s)}{4}$$

During S3:

$$V_{L\_boost1} = V_{in} - V_x - V_y - V_B - V_S$$
$$V_{L\_boost2} = V_{in} - V_x + V_y - V_B - V_S$$
$$V_{L\_boost3} = V_{in} + V_x - V_z - V_{out} - V_B - V_T - 2V_S$$
$$V_{L\_boost4} = V_{in} + V_x + V_z - V_B - 2V_S$$

$$V_{L\_boost1} - V_{L\_boost2} = -2V_y = 0 \Rightarrow V_y = 0$$
$$V_{L\_boost3} - V_{L\_boost4} = -2V_z - V_{out} - V_T = 0 \Rightarrow V_z = \frac{-(V_{out} + V_T)}{2}$$
$$V_{L\_boost1} - V_{L\_boost4} = -2V_x - V_z + V_s = 0 \Rightarrow V_x = \frac{V_{out} + V_T + 2V_s}{4}$$

During S4:

$$V_{L\_boost1} = V_{in} - V_x - V_y - V_B - V_S$$
$$V_{L\_boost2} = V_{in} - V_x + V_y - V_B - V_S$$
$$V_{L\_boost3} = V_{in} + V_x - V_z - V_B - 2V_S$$
$$V_{L\_boost4} = V_{in} + V_x + V_z - V_{out} - V_B - 2V_S - V_T$$

$$V_{L\_boost1} - V_{L\_boost2} = -2V_y = 0 \Rightarrow V_y = 0$$
$$V_{L\_boost3} - V_{L\_boost4} = -2V_z + V_{out} + V_T = 0 \Rightarrow V_z = \frac{V_{out} + V_T}{2}$$
$$V_{L\_boost1} - V_{L\_boost4} = -2V_x - V_z + V_{out} + V_s + V_T = 0 \Rightarrow V_x = \frac{V_{out} + V_T + 2V_s}{4}$$

So $V_{L\_boost1}=V_{in}-V_B-V_S$ during S0 and $V_{L\_boost1}=V_{in}-V_{out}/4-V_T/4-V_B-3V_S/2$ during S1, S2, S3 and S4
The duration d0 of S0 is (d-3/4)T and the duration d1 of S1 is (1-d)T. In steady state mean voltage over the inductor is zero during a period, therefore we can write:

$$\left(3/4 - d\right)\left(V_{in} - V_B - V_S\right) = \left(1 - d\right)\left(V_{in} - V_{out}/4 - V_T/4 - V_B - 3V_S/2\right)$$

Rewriting the above equation leads to:

$$V_{out} = \frac{1}{1-d}\left(V_{in} - V_B\right) - V_T - \left(\frac{3-2d}{1-d}\right)V_S$$

During S0 the voltage over L_{boost1} is lower, so the ripple is less with resistances then without resistances.

3.2 Distribution of power over the branches caused by component tolerances

In the preceding paragraph it was shown that non-ideal components lead to changed characteristics for the output voltages and different ripple currents in the branches, but when the parasitic components are equal in all branches the current will still be equally divided over the four branches.
In practice however there will be differences between the branches. For example the duty cycles won't be equal in all branches. The $R_{ds,on}$ of the MOSFETs will be different and also the parasitic resistances of the boost inductors and the input transformers will differ. In this paragraph the influences of differences in on-resistance of the MOSFETs and differences in duty cycles on the distribution of the current will be investigated.

The circuit that will be used for this investigation can bee seen in figure 15.

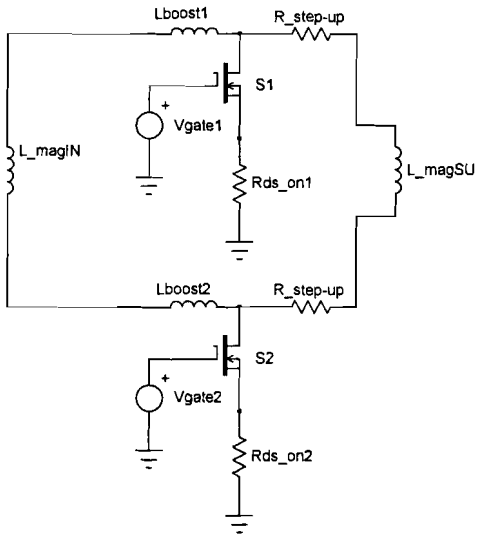

Figure 15: Circuit to investigate current distribution deviation caused by tolerances in the circuit.

In the preceding paragraph the voltage over the magnetizing inductance of the input transformer was a square wave voltage with a mean value of zero volts. The magnetizing inductance is the only path for a differential current; when the mean voltage over it is zero there will be no differential current.
When there is a mean voltage over the inductance there will be a rising differential current and the current won't be equally distributed over the branches anymore.
The drain voltage of S1 will be called V_{S1} and the drain voltage of S2 will be called V_{S2}.
The voltage difference between V_{S1} and V_{S2} will be investigated and so the steady state magnetizing current, which equals the differential current can be calculated.
The current through L_{boost1} will be called I_1 and the current through L_{boost2} will be called I_2.
There are three different states for the circuit: during S0, from time 0T to $(d_2-0.5)T$ and from 0.5T to d_1T, both switches are closed, during S1 from time d_1T to 1T, only switch S1 is open and during S2, from $(d_2-0.5)T$ to 0.5T, only switch S2 is open.
The output voltage of the system is $V_{out} = \frac{1}{1-d_{max}} V_{in}$ in which $d_{max}=\max(d_1,d_2)$
First the system will be described during each state.

During S0:

$$V_{S1,0} = I_1 R_{ds,on1}$$

$$V_{S2,0} = I_2 R_{ds,on2}$$

$$V_{S2,0} - V_{S1,0} = I_2 R_{ds,on2} - I_1 R_{ds,on1}$$

During S1:

$$V_{S1,1} = I_1 2R_{step\_up} + (I_1 + I_2)R_{ds\_on2} + V_{out}$$
$$V_{S2,1} = (I_1 + I_2)R_{ds,on2}$$
$$V_{S2,1} - V_{S1,1} = -(I_1 2R_{step\_up} + V_{out})$$

And during S2:

$$V_{S1,2} = (I_1 + I_2)R_{ds,on1}$$
$$V_{S2,2} = I_2 2R_{step\_up} + (I_1 + I_2)R_{ds\_on1} + V_{out}$$
$$V_{S2,2} - V_{S1,2} = I_2 2R_{step\_up} + V_{out}$$

Now one can write:

$$V_{S2} - V_{S1} =$$
$$= (d_2 - 0.5)(V_{S2,0} - V_{S1,0}) + (1 - d_2)(V_{S2,2} - V_{S1,2}) + (d_1 - 0.5)(V_{S2,0} - V_{S1,0}) + (1 - d_1)(V_{S2,1} - V_{S1,1})$$
$$= (d_1 + d_2 - 1)(V_{S2,0} - V_{S1,0}) + (1 - d_1)(V_{S2,1} - V_{S1,1}) + (1 - d_2)(V_{S2,2} - V_{S1,2})$$
$$= (d_1 + d_2 - 1)(I_2 R_{ds,on2} - I_1 R_{ds,on1}) - (1 - d_1)(I_1 2R_{step\_up} + V_{out}) + (1 - d_2)(I_2 2R_{step\_up} + V_{out})$$

When the duty cycles are equal and only the resistances of the MOSFETs differ this leads to:

$$V_{S2} - V_{S1} = (2d - 1)(I_2 R_{ds,on2} - I_1 R_{ds,on1}) + (1 - d)(I_2 - I_1)2R_{step\_up}$$

In steady state, the voltage over the magnetizing inductance is zero and the above equation reduces to:

$$(2d - 1)(I_2 R_{ds,on2} - I_1 R_{ds,on1}) = (1 - d)(I_1 - I_2)2R_{step\_up}$$

By substituting I_1-I_2=I_{mag} and $R_{ds,on2}$=(1+k)$R_{ds,on1}$, which means that k is the relative difference between the on resistances, this can be rewritten as:

$$(2d - 1)R_{ds,on1}(I_{mag} + kI_2) = -(1 - d)I_{mag} 2R_{step\_up}$$
$$\Rightarrow I_{mag}\{(2d - 1)R_{ds,on1} + (1 - d)2R_{step\_up}\} = -kI_2 R_{ds,on1}(2d - 1)$$
$$\Rightarrow I_{mag} = \frac{-kR_{ds,on1}(2d - 1)I_2}{(2d - 1)R_{ds,on1} + (1 - d)2R_{step\_up}}$$

Because 1-d is positive the magnetizing current is smaller than $-kI_2$, when one assumes that the on resistance of the MOSFETs is much larger than the resistance of the step-up transformer windings the magnetizing current equals $-kI_2$, this is the worst case magnetizing current. One can now write:

$$I_{in} = I_1 + I_2 = 2I_2 + I_{mag} \Rightarrow I_{mag} \le \frac{-k}{2-k} I_{in}$$

And because k is small compared to 2:

$$I_{mag} \le -k\frac{I_{in}}{2}$$

A small difference in resistances leads to a small difference in the currents, but not to insuperable problems. Each branch should be designed for (1+k) times the expected power.

When the resistances are equal and only the duty cycles differ, one can write:

$$V_{S1} - V_{S2} =$$
$$(d_1 + d_2 - 1)(I_2 R_{ds,on} - I_1 R_{ds,on}) - (1 - d_1)(I_1 2R_{step\_up} + V_{out}) + (1 - d_2)(I_2 2R_{step\_up} + V_{out})$$

When one substitutes $d_2=d_1(1+k)$, which means that k is the relative difference in the duty cycles, this becomes:

$$V_{S1} - V_{S2} = (2d_1 + d_1 k - 1)(I_2 - I_1)R_{ds,on} + (1 - d_1 k)(I_2 - I_1)2R_{step\_up} + d_1 k V_{out}$$

In steady state the voltage over the magnetizing inductance is zero.

$$d_1 k V_{out} = (2d_1 + d_1 k - 1)(I_{mag})R_{ds,on} + (1 - d_1 k)(I_{mag})2R_{step\_up}$$

$$\Rightarrow \frac{d_1 k}{1 - d_1 - d_1 k} V_{in} = I_{mag}\{(2d_1 + k d_1 - 1)R_{ds,on} + (1 - d_1 k)2R_{step\_up}\}$$

$$\Rightarrow I_{mag} = \frac{d_1 k}{\{1 - d_1 - d_1 k\}\{(2d_1 + k d_1 - 1)R_{ds,on} + (1 - d_1 k)2R_{step\_up}\}} V_{in}$$

When $d_1 k$ is neglected in the denominator this can be rewritten as:

$$I_{mag} = \frac{d_1 k}{(2d_1 - 1)R_{ds,on} + 2R_{step\_up}} V_{out}$$

The input current of the converter is very large. To avoid very large resistive losses the resistances of the MOSFETs and the step-up transformers are very low. This leads however to enormous magnetizing currents, when there is a small difference in duty cycle, and saturation of the input transformers. All power will be provided by one branch and the power won't be distributed over the four branches anymore. In addition, the frequency of the current in the branch is equal to the switching frequency and not four times the switching frequency anymore.

One has to make sure that there is only a very small difference in duty cycle between the branches. A duty cycle difference of 1 % at a duty cycle of 0.8, which leads to an output voltage of 100 V, with $R_{ds,on}$ = 20 mΩ and $2R_{step\text{-}up}$ = 6 mΩ already leads to a magnetizing current of more than 40 A. When one also takes into account the resistances of the input transformer and the boost inductor this magnetizing current will drop to about 25 A. One branch will generate 1 kW and the other one no power at all. Therefore, instead of four branches designed for one quarter of the input power one has to design four branches for half the input power. Also the input transformer that will not saturate at a magnetizing current of 25 A will be very big. Building such a converter without a control that makes all the currents equal by altering the duty cycles will lead to a very low power density.

4 Realizing the PEMFC DC-DC converter

Now the operation of the converter is known, one can start realizing it.
The converter consists of one input transformer that divides the input current in two, two input transformers that divide half the input current in two again, four boost inductors, four switches, two step-up transformers, 8 diodes and a circuit to control the switches one by one, shifted in time.

First, all the component values will be calculated. After that, every component will be designed one by one.

4.1 Calculating the component values

The boost converter amplifies the input voltage from 20 V to 100 V, so the duty cycle is 0.8.
The switching frequency is 100 kHz, so the switching period is 10 µs.
The input power is 2 kW, so the input current is 100 A.
The current input ripple is 5 %, so the peak-peak current ripple is 5A.
With eq. (5) one can calculate the boost inductance:

$$L_{boost} = \frac{V_{in}(4d-3)T}{\Delta I_{in}} = \frac{20*(4*0.8-3)*10*10^{-6}}{5} = 8\mu H$$

Because of the resistive losses, the duty cycle might have to be higher. This will increase the ripple current and the boost inductor was chosen to be 10 µH. The expected ripple current is now 4 A.

The current ripple in the branches caused by the boost inductors, that can be calculated by eq. (6), is very small, 1 A. Now one can calculate the magnetizing inductance of the input transformers by restricting the ripple current in the branches.
The maximum magnetizing current is the maximum ripple current in a branch minus the ripple current caused by the inductor. This is 5-1=4 A:

$$I_{mag,\max} = \frac{V_x}{L_{mag1}}(1-d)T + \frac{V_y}{L_{mag2}}(1-d)T = \frac{V_x+V_y}{L_{mag}}(1-d)T = \frac{3/4\,V_{out}}{L_{mag}}(1-d)T$$

This is valid when both magnetizing inductances are equal.

One can now calculate the magnetizing inductance:

$$L_{mag,\min} = \frac{3/4\,V_{out}(1-d)T}{I_{mag,\max}} = \frac{75*2*10^{-6}}{4} = 38\mu H$$

There will also be a magnetizing current in the step-up transformers.

One branch should transfer 500 W, with an output voltage of 400 V this means a mean output current of 1.25 A. The current however only flows during (1-d)T so the output current will be 6.25 A during 0.2T. The transformer amplifies the voltage from 100 V to 400 V so the turns ratio is 4. The primary current will then be 4*6.25=25 A. The magnetizing current of the transformer will be limited to 5 % of 25 A, that is 1.25 A. This leads to a magnetizing inductance of:

$$L_{mag,step\_up,\min} = \frac{100}{2.5}2*10^{-6} = 80\mu H$$

The resistive power loss in the MOSFETs is $4*I^2R$. When one approximates the current through the MOSFET to be 25 A and allows 2.5 % resistive losses in the MOSFETs, the maximum allowed $R_{ds,on}$ will be 20 mΩ.

4.2 Designing the components

Now the component values are known, the right ones can be chosen. Transformers and inductors however don't come ready made but have to be designed by oneself. Within Philips, this is usually done with the MagTool software.

4.2.1 The input transformers

Because of the nearly ripple less current solid wire can be used for this transformer. First, a design was made in MagTool, but after consulting the passive component engineer of PDC, one decided that thick solid wire around an e core isn't feasible. The component engineer recommended the use of a toroidal core with high permeability material. Because of the toroidal shape, the solid wire can easily be wound and brought out of the transformer for connection and the high permeability material leads to a small amount of windings and therefore a small resistance of the windings considering the resistive losses in the transformer.
These cores however aren't implemented in MagTool.
The number of windings was calculated with: $n = \sqrt{L_{mag} / A_L}$, in which A_L is a value that can often be found in the datasheet of the core.
The same area of copper was used compared to the MagTool design.
A transformer was build using a toroidal core with an output diameter of 25.25 mm made of 3E5 material. The windings consisted of 4 wires of 1.3 mm^2 in parallel and each winding consisted of 3 turns. The transformers in the second stage for the smaller current were made with the same core and the same number of windings, but with 2 parallel windings instead of four, because of the lower current through the windings.
During testing however these transformers saturated very quickly because of a small duty cycle difference between the branches.
After that nanocrystalline material was used for the cores, first small cores but when these became too hot, bigger ones were used.
The cores became hot because of the Volt second product that is applied to it. The program that the component engineer suggested to design the transformer with is to design common mode filter inductors, as there are no core losses in common mode filters on the contrary to the input transformers.

So finally, for the input transformers toroidal cores were used of nanocrystalline material.
The cores were from VACUUMSCHMELZE GMBH. The material is VITROPERM 500 F.
For the first transformer a core with an outside diameter of 32.3 mm was used and for the other two one used cores with an outside diameter of 42.3 mm, the windings were unchanged. It might be that for all transformers the cores of 32.3 mm can be used, but three cores weren't available. This should be looked at in the future.
The design data from the Magnetics Common Mode Filter Inductor Design program can be seen in Appendix A1.

4.2.2 The boost inductors

The current through the boost inductors has hardly any ripple. It has a very high mean value of 25 A.
The ripple-less very high current is the reason why one chose to use High Flux cores. This material has a very flat saturation curve and can therefore operate with very high flux density, which reduces the number of windings that is needed for the inductor.
The inductor was designed using the Magnetics DC Inductor Design software by Magnetics Inc.
This program calculates the wire size in AWG. The area of the wire was 2.6 mm^2 and this is realised by using 2 wires of 1.3 mm^2 in parallel.
In Appendix A2 one can see the design data from the design software. Here one can see the influence of the flat saturation curve. At no load the inductance is 19 μH and at full load it is only 10 μH.

4.2.3 The step-up transformers

The step-up transformer is very similar to the isolation transformer designed during a former traineeship [5]. It amplifies the voltage from 100 V to 400 V and has a build in isolation function because there is a distance between primary and secondary winding. This transformer is designed with MagTool, using a PQ50 core. In the former traineeship one core was used for a 2kW transformer, but here the frequency of the current is higher. There will be more proximity losses and core losses so two PQ50 cores are needed to be able to transfer the heat.

In the previous chapter the magnetizing current that could flow because of a duty cycle difference was calculated. The voltage difference on the drains of the MOSFETs will also cause a DC magnetizing current through the step up transformers, which will probably saturate because of that. To prevent a DC current from flowing through the transformers DC blocking capacitors are placed in front of the transformers.

Because of the distance between the primary and secondary winding there will be a leakage inductance [5]. This leakage will limit the current drop in the diodes when the MOSFET is turned on. This will limit the reverse recovery losses in the diodes.

The design data of the step-up transformer can be found in Appendix A3

4.2.4 The MOSFETs

The boost converter amplifies the input voltage to 100 V. Because of parasitic components in the circuit, there will be some oscillation in the circuit and therefore 150 V MOSFETs were chosen.

In the previous paragraph the maximum $R_{ds,on}$ was calculated to be 20 mΩ. When one chooses to use Philips MOSFETs, this leaves only two options; one can use the PSMN020-150 or one can use two PSMN030-150 in parallel. The on resistance of MOSFETs increases 70 % at maximum operating temperature so then the PSMN020 can have a too high resistance. In addition, the PSMN020 is not available in surface mountable device (SMD) package while the PSMN030 is. Therefore, one chose to use two PSMN030 devices in parallel.
The data sheet of this MOSFET can be found in Appendix B1.

4.2.5 The diodes

Because of the similarity between the rectifiers used in the isolation stage [5] and in this PEMFC DC-DC converter the same diodes are used. This is the Philips BYV29X-600.
The data sheet of this diode can be found in Appendix B2.

4.2.6 Snubber circuits

When the MOSFET is turned on the current through Lboost will also go flow through the MOSFET, when it is switched off the current has to flow through Lleak. The step in the current through Lleak will cause an infinite voltage on the drain of the MOSFET can cause damage to the MOSFET. The peak voltage snubber over the MOSFET to limit the maximum drain voltage can be seen in figure 16.

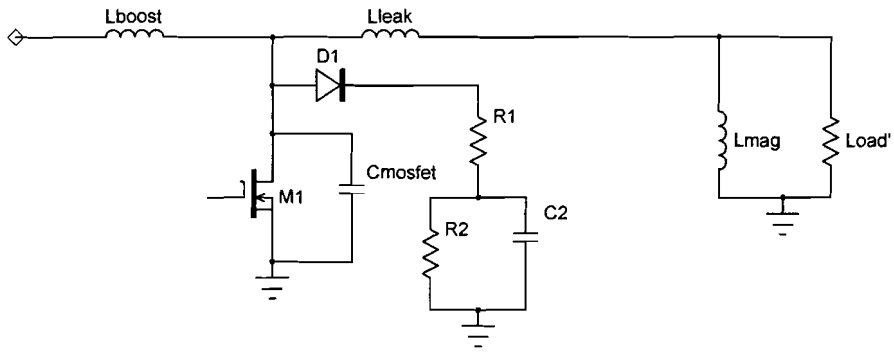

Figure 16: The MOSFET with a peak voltage snubber.

When M_1 is opened the boost current cannot flow directly through the leakage inductance. First the current will charge C_{mosfet} and the drain voltage will rise. When the drain voltage becomes higher than the voltage over C_2, which is V_B, the diode D_1 starts to conduct and clamps the drain voltage.
The current through the diode will charge the capacitor C_2 up to the voltage V_E untill the current is taken over by the leakage inductance. The resistor R_1 is placed to damp the oscillation caused by L_{leak} and C_2.
When the diode stops to conduct, the capacitor C_2 is discharged through R_2 and the voltage over it will decrease from V_E to V_B again.
During the discharging of the capacitor C_2 energy will be dissipated in resistance R_2. This energy is not delivered to the output of the converter and contributes to the losses in the circuit.

The energy dissipated in the discharging resistance can be calculated by:

$$E = \frac{1}{2}CV_E^2 - \frac{1}{2}CV_B^2 = \frac{1}{2}C\left(V_E^2 - V_B^2\right)$$

This leads to a power loss in the resistor of E*f and to a power loss in the snubber of:

$$P_{loss} = \frac{1}{2}C\left(V_E^2 - V_B^2\right)f$$

By substituting an end voltage, V_E, of 100 V, a begin voltage, V_B, of 95 V, the switching frequency of 100 kHz and a power loss in the snubber of 2 W one can calculate the wanted capacitance to be 40 nF. During dT the capacitance should be partially discharged so the voltage over it goes from 100 V to 95 V. The discharging takes place through resistor R2 and one can write:

$$\Delta Q = I\Delta t = \frac{V}{R}dT = \frac{100}{R} * 8 * 10^{-9} = C\Delta V = 40 * 10^{-9} * 5$$

And now one can calculate R2 to be 4kΩ. R1 has to be small or else the charging current through it will higher the drain voltage, but if it is too small the damping will be too small and there will be an oscillation on the drain voltage. R1 was chosen, during operation of the system at 400W, to be 20 Ω.

The above-mentioned snubber suppresses oscillations during switch off of the MOSFET, during switch on of the MOSFET the diode is turned off and the parasitic capacitance of the diode causes oscillation in the circuit. This is solved by placing a series connection of a resistor and a capacitor over the diode like in figure 17.

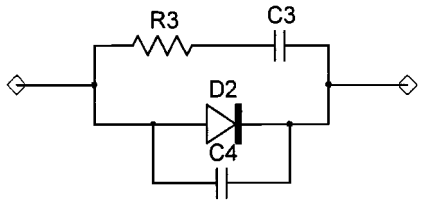

Figure 17: The diode with a dV/dt snubber.

The capacitor C3 lowers the frequency of the oscillation and the resistor R3 damps the oscillation. During the (dis)charging of C3 energy is being dissipated in the resistor R3. This energy contributes to the losses in the circuit.

The energy dissipated in the resistor during charging and discharging of the capacitor C3 can be calculated by $E = C(\Delta V)^2$, this leads to a power loss of $P = C(\Delta V)^2 f$. Limiting the power in the snubber to 2 Watts leads to a capacitor of 120 pF. Resistor R3 can't be too big because then it decouples C3 from the system and can't be too small because then it won't damp the oscillation. The resistor R3 was chosen, during operation of the system at 400 W, to be 750 Ω.

4.2.7 The MOSFETs control circuit

The four boost switches will be controlled by four ON Semiconductor MC33023 Voltage Mode PWM ICs (see Appendix C). These ICs were chosen because they have an input pin for synchronisation. As was mentioned before the four switches have to be controlled shifted T/4 in time.
To generate four time shifted control signals, first an oscillator is build using a 555 IC to generate an oscillating signal with four times the switching frequency. This signal is send into the clock input of a Philips 74HC107 JK-flip-flop with both J and K connected to the positive supply voltage. The 2 output signals Q1 and INV(Q1) now are oscillating signals, which are 180 degrees out of phase. These two signals are again frequency divided using two JK-flip-flops to become four signals at the switching frequency, which are T/4 shifted in time. These signals however have a duty cycle of 50 % and only a short positive pulse is needed. This is reached by using the signal at the switching frequency, twice the switching frequency and the inverted output signal of the 555 as inputs of a 3 input AND IC (Philips 74HC11). The output signal of the 555 and the output signals of the 3 flip-flops can be seen in figure 18.

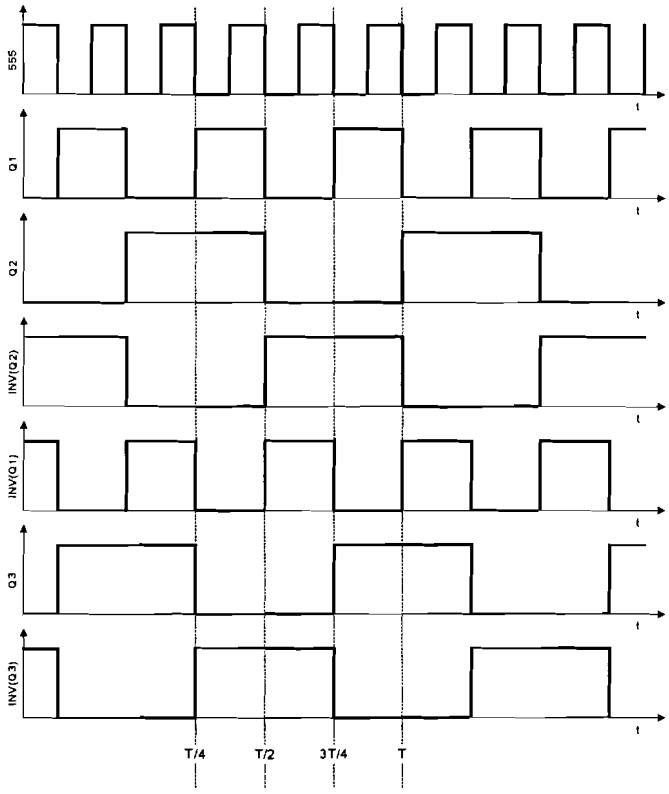

Figure 18: Oscillating signals at once, twice and four times the switching frequency.

The MC33023 is an IC that would be used for a closed loop circuit. A signal that is representative for the output voltage would be used to control the duty cycle to reach the wanted output voltage. During this traineeship however the circuit was operated in open loop and the "feedback" voltage was derived from the supply voltage using a potentiometer.

The MOSFETs have a large input capacitance. A large current should be supplied by the control ICs. A gate drive circuit is used to supply this current. The gate drive circuit can be seen in figure 19.

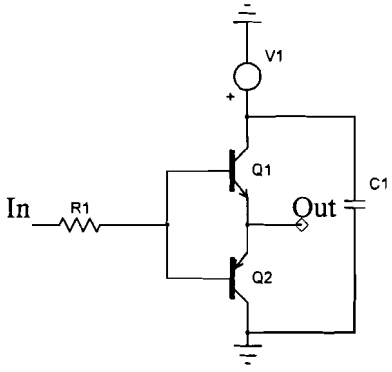

Figure 19: Gate drive circuit.

4.3 The realised system

A breadboard of the system was build. Below one can see two pictures of the breadboard.

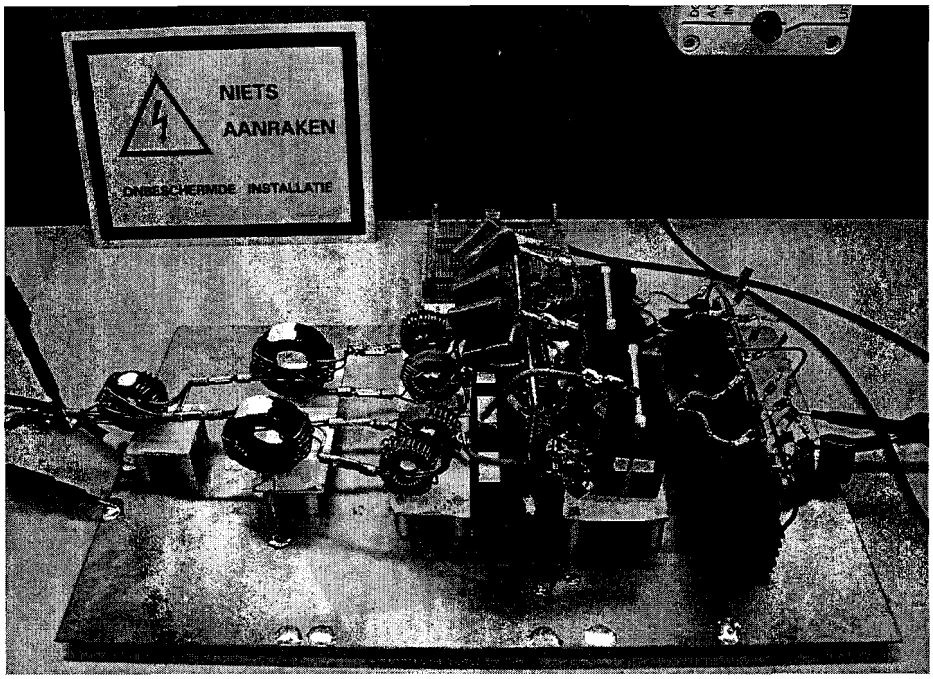

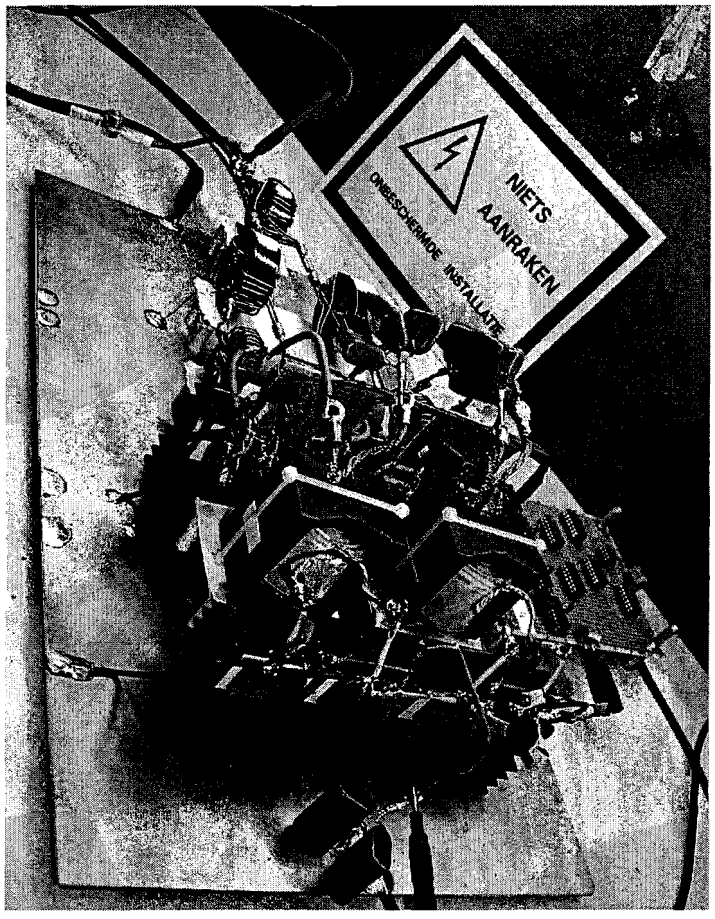

5 Testing the PEMFC DC-DC converter

After the system was build, the operation was tested. First the signals in the system were checked to see if they matched the simulation results. After that the losses in the converter were measured. These measured losses will be compared with the predicted losses.

5.1 Circuit signals during operation of the converter

In this paragraph the circuit signals during operation will be compared with the measured signals during operation. First the system was simulated in ICAP Spice and after that the signals were measured on the breadboard.

5.1.1 Simulation of the converter

First the system was simulated. The circuit that was simulated can be seen in figure 20. In the figures 21 and 22 one can see the simulation results.

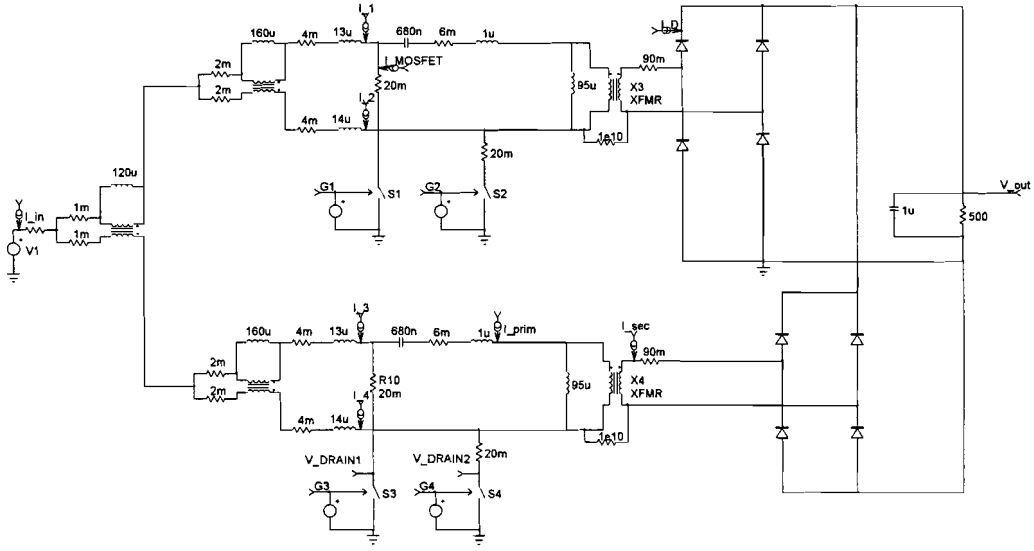

Figure 20: Simulated circuit of the PEMFC converter. The transformers x, y and z have a turns ratio of minus 1.

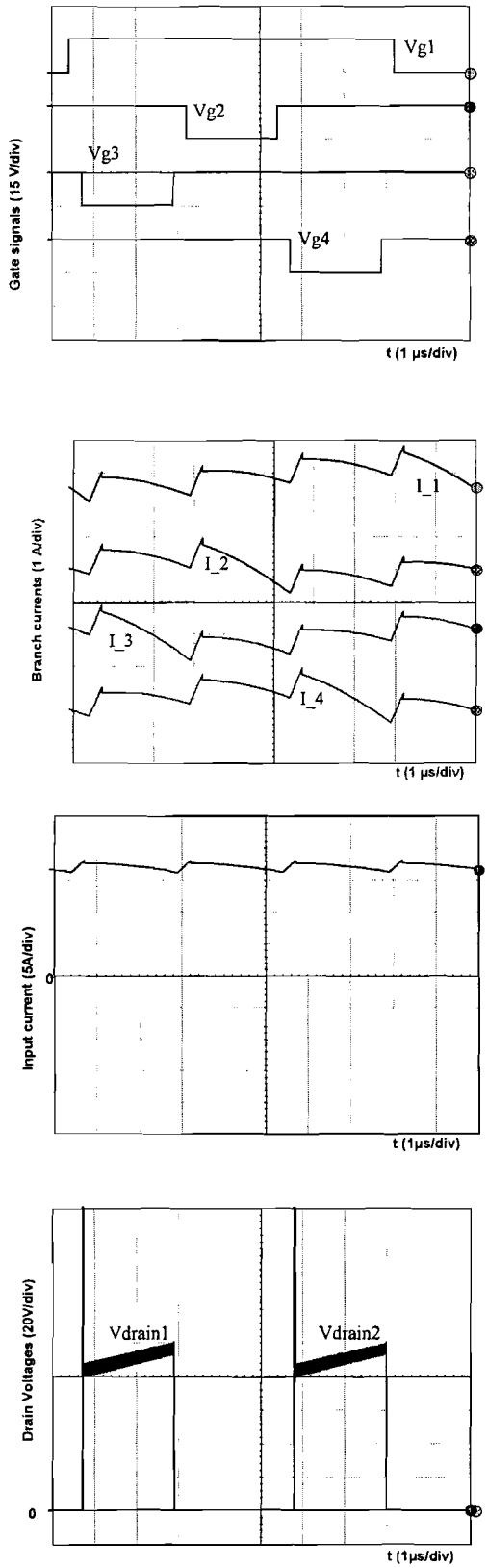

Figure 21: Simulation results of the PEMFC converter.

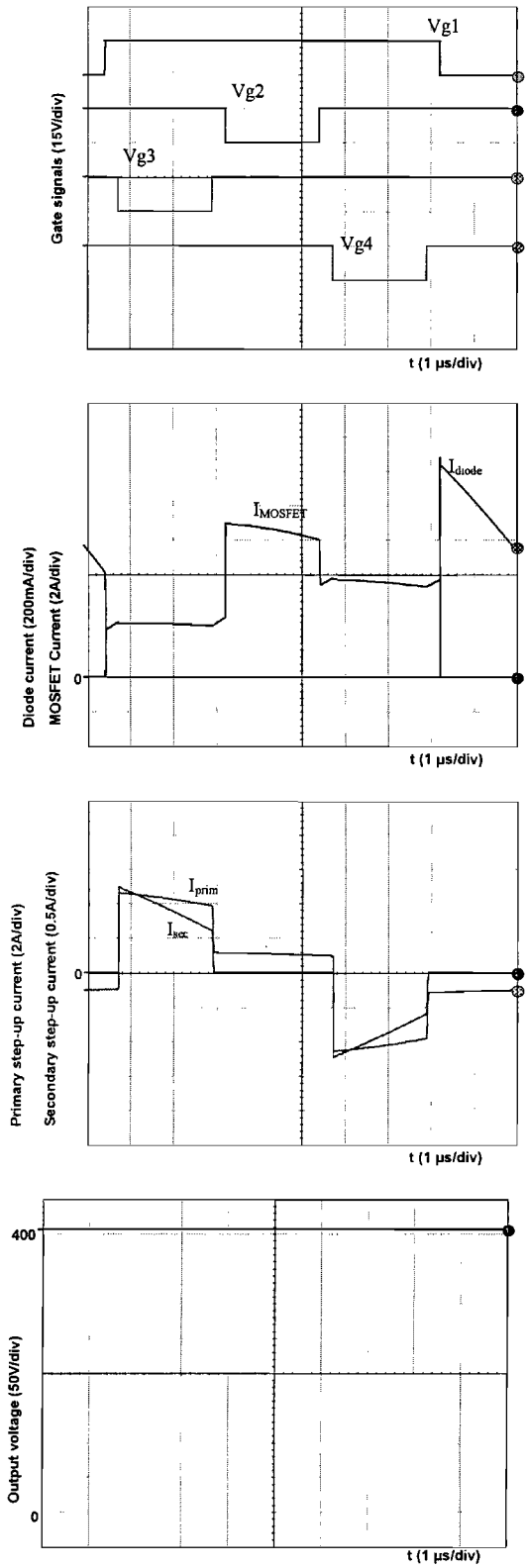

Figure 22: Simulation results of the PEMFC converter.

5.1.2 Measured signals of the converter

The system was operated with a resistive load of 498 Ω. The input voltage was 19.8 V and the output voltage 404 V. In figure 23 one can see the measured signals.

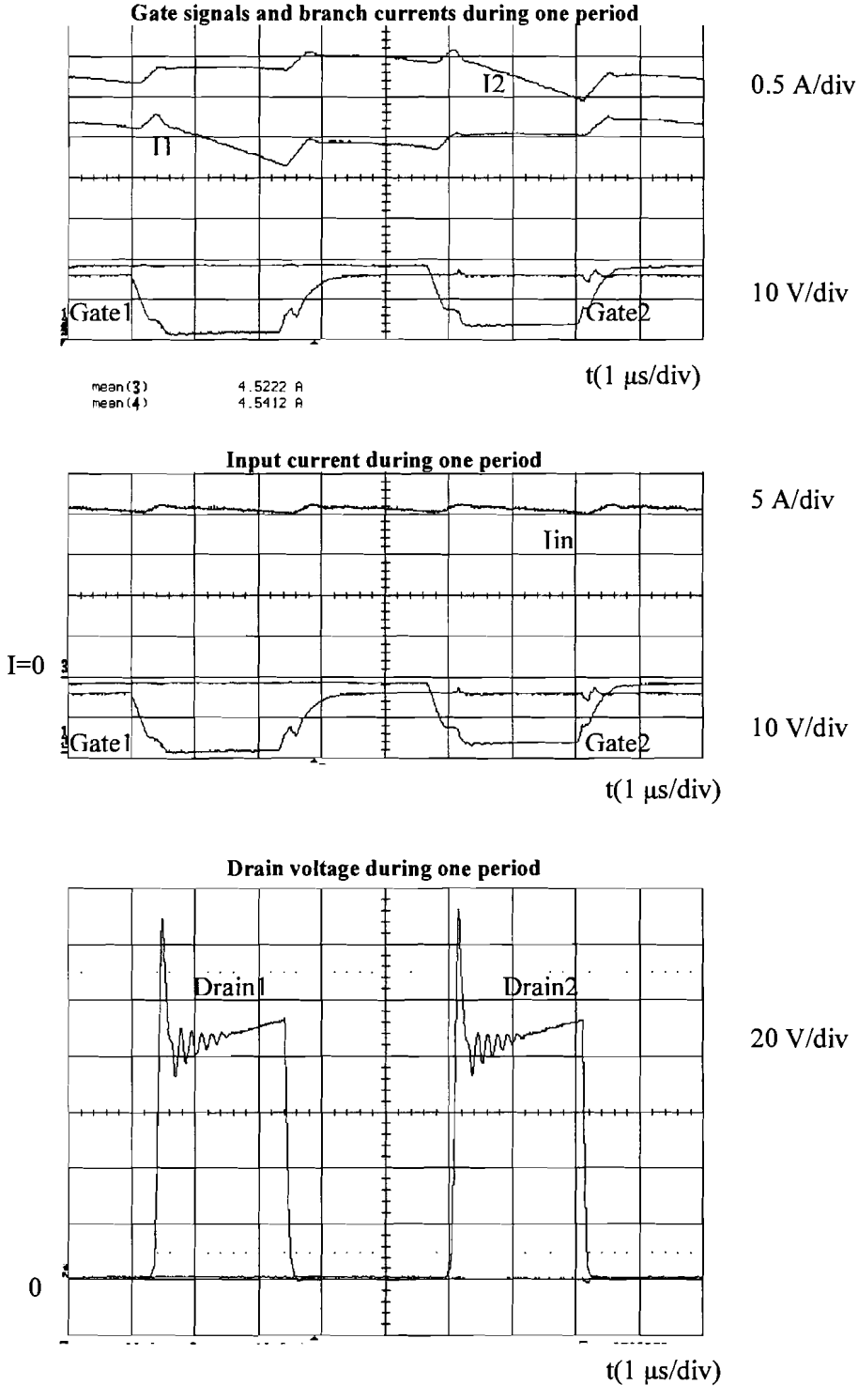

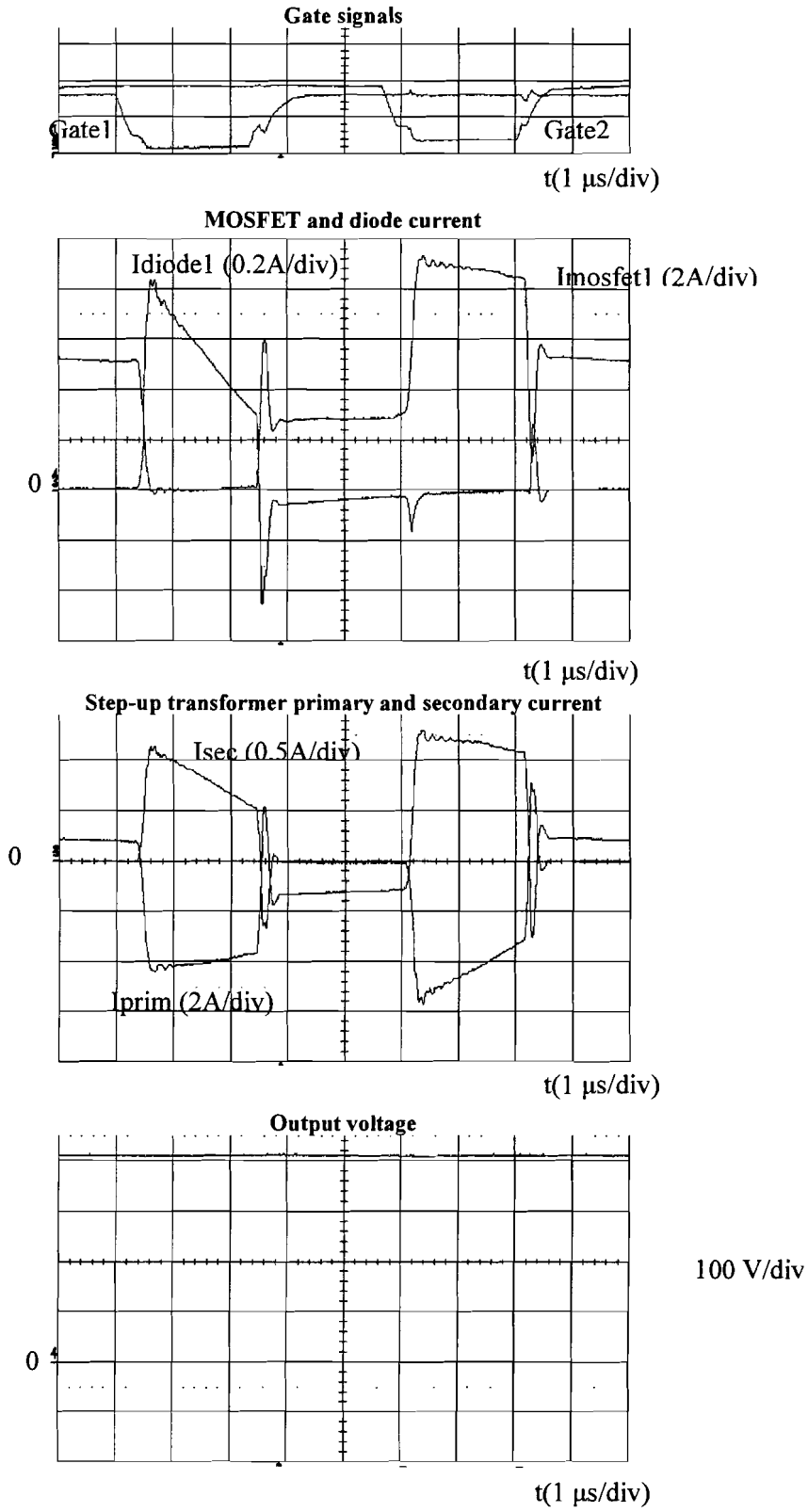

Figure 23: Measured signals of the PEMFC converter.

5.1.3 Comparing the simulation to measurement results

The simulated signals will be described and they will be compared to the measured signals.

In the simulation the gate signals are generated by voltage sources and the gates of the MOSFETs don't have capacitances. During the measurement the gates have capacitances and this causes the rise and fall of the gate voltage to be limited.

The measured branch currents have a smaller ripple than the simulated currents. During the simulation the boost inductance is 10 μH, however the inductance during the measurement is higher because of the flat saturation curve. The inductance at no load is 19 μH and at nominal load it is 10 μH. During this measurement it will be somewhere in between, but close to 19 μH.

The expected input ripple can be calculated with eq. (5), in which the boost inductance will be 19 μH and the switching frequency will be 107 kHz, to be 2.0 A. The measured ripple from figure 23 is 0.35(div)*5(A/div) = 1.8 A. The ripple is hard to read from the figure so the tolerance on the measured figure is high. The measured ripple is however very comparable to the expectations. The small difference might be explained by a small decrease of the boost inductance caused by the DC current through it.
The expected ripple current in the branches consists of one quarter of the input ripple and the ripple caused by the magnetizing inductances of the input transformers and the step-up transformer. The calculated ripple is 1.3 A and the measured ripple is 1.6 A. Probably this small difference is caused by lower magnetizing inductances of the transformers which explain the higher ripple current.

When the MOSFET is switched off the boost inductor current wants to flow through the leakage inductance of the step-up transformer, when the MOSFET was switched on only the magnetizing current of the step-up transformer was flowing through it. This step in current will cause an infinite voltage on the drain during the simulation and causes the dip in the branch current. This can also be seen in the measurements, but the peak snubber limits the drain voltage and the current drop is less.

Another phenomenon is the rising drain voltage after the peak. This is caused by the DC blocking capacitor. The constant current through the capacitor causes a rising voltage. This can be seen in both the simulation and the measurements.

When one looks at the MOSFET current during simulation and compares this with the ideal current from figure 10, one can see that during simulation there is a difference in the MOSFET current before and after the off period of the other MOSFET. This is caused by the magnetizing current through the step-up transformer. The magnetizing current during this simulation seems large but at full power it will only be 5 % of the total current.
One can see that, however the diode current is on the secondary, low current, side of the transformer and the leakage inductance of the transformer limits the current drop, there still is a noticeable reverse recovery current. This reverse recovery current flows through the MOSFET on the primary side of the transformer and causes extra losses.

When one looks at the simulation of the step-up transformers' primary and secondary currents one notices again the magnetizing current mentioned before. When one switch is open the magnetizing current will change from positive to negative, or the other way around, with a constant slope. This causes the difference in slope between the primary and secondary current.

One can say that the measurements compare well with the simulations, and that the model is in good agreement with the realised converter. The one thing that attracts the most attention is the reverse recovery current that will cause extra losses in the circuit.

5.2 Efficiency of the converter

In this paragraph first the sources of losses are mentioned and the expected losses are calculated for input currents of 37 A and 100 A. Then the losses are measured for various input powers and an estimation for the efficiency of the converter at full power is given. At 800 W the measured losses are compared with the expected losses.

5.2.1 Sources of losses in the converter

There are several losses in the converter:

- resistive losses in input transformers, boost inductors, MOSFETs and step-up transformers,
- core losses in input transformers, boost inductors and step-up transformers,
- proximity losses in the step-up transformers,
- losses caused by the leakage inductance of the step-up transformers,
- switching losses in the MOSFETs and diodes,
- forward losses in the diodes and
- losses in the snubbers.

All these losses will be evaluated in this paragraph.

Resistive losses

The branch current is nearly ripple-less and can be considered constant; it flows through the input transformers and boost inductors winding resistances and the losses can be calculated by:

$$P = 4I_{branch}{}^2 R_{winding}$$

The current through a MOSFET is I_{branch} during (2d-1)T, 2 I_{branch} during (1-d)T and zero during (1-d)T. The resistive losses in MOSFET are:

$$P = 4I_{MOSFET}{}^2 R_{ds,on} = 4\left\{(2d-1)I_{branch}{}^2 + (1-d)4I_{branch}{}^2\right\}R_{ds,on} = 4(3-2d)I_{branch}{}^2 R_{ds,on}$$

The current through the step-up transformer is I_{branch} during 2(1-d)T and zero the rest of the time. The losses in the windings are:

$$P = 2I_{step-up}{}^2 R_{winding,su} = 4(1-d)I_{branch}{}^2\left(R_{prim} + \frac{R_{sec}}{n^2}\right)$$

The current in one branch is the input current divided by four and one can write for the total resistive losses:

$$P = \frac{1}{4}I_{in}{}^2\left\{R_{winding} + (3-2d)R_{ds,on} + (1-d)\left(R_{prim} + \frac{R_{sec}}{n^2}\right)\right\}$$

Core losses

The core losses in the input transformers can be estimated with the Steinmetz formula [9].
The core losses per kg are given by:
$P=C_m * f^x * B_{max}{}^y$.
The factors x and y can be calculated by filling in values from the data sheet of the cores. The data sheet can be found in Appendix C

The core losses in the boost inductors can be neglected because the branch current is nearly ripple-less.

The core losses in the step-up transformers can be simulated in MagTool.

Proximity losses

There are only proximity losses in the step-up transformers since the currents in the other magnetic components are nearly ripple-less. These losses can be simulated in MagTool.

Losses caused by the leakage inductance of the step-up transformers

When the current is flowing through the step-up transformer there will be an energy $\frac{1}{2}L_{leak}I_{branch}^2$ in the leakage inductance. When the MOSFET is turned on the current through the transformer will be zero and the energy in the inductance will be dissipated in the MOSFET. The dissipation of the energy leads to a loss of:

$$P = 4 * \frac{1}{2} * L * I_{branch}^2 * f = 2L\left(\frac{I_{in}}{4}\right)^2 f = \frac{1}{4} I_{in}^2 \left(\frac{1}{2} Lf\right)$$

Switching losses

As can be seen in the previous paragraph there is a reverse recovery current through the diodes. This current is transferred to the primary side of the transformer where it causes losses in the MOSFETs these losses can be approximated by $Q_{rr}*n*V*f$. Qrr can be found in the data sheet of the diode n is the transformer ratio, V is the drain voltage of the MOSFET, which is 100 V and f is the switching frequency. There are eight diodes in the circuit and these all cause reverse recovery losses.

Forward losses

During (1-d)T the current $\frac{1}{4}I_{in}/n$ flows through two diodes on the secondary side of the transformer, this causes forward losses in the diodes.
The total losses in all eight diodes can be calculated by:
$P=8*(1-d)*\frac{1}{4}*I_{in}/n*V_f=2*(1-d)*I_{in}/n*V_f$
The forward voltage can be found in the data sheet of the diode, it is 1 V.

Snubber losses

The peak voltage snubber over the MOSFET is used to suppress the peak voltage on the drain when the MOSFET is switched off. The energy $\frac{1}{2}C(V_e^2-V_b^2)$ will be dissipated in the discharging resistor after turning on the MOSFET. The power loss caused by the four peak voltage snubbers is $2\ C(V_e^2-V_b^2)$.

The power loss in the snubber over the diode is $\frac{1}{2}CV^2f$, that is $4CV^2f$ in 8 diodes.

Calculation of expected losses when I_{in} is 37 A

$R_{winding}$ is 7 mΩ, $R_{ds,on}$ is 20 mΩ, R_{prim} is 6 mΩ, R_{sec} is 90 mΩ and n is 4.5. The expected resistive losses are **15 W**.

The frequency in transformer x is 200 kHz and in transformer y and z it is 100 kHz. The measured B_{max} is 140 mT in both cores. The flux density, B, is calculated by integrating the flux derivative that is measured with extra windings around the core and assuming that the average flux is zero. The magnetic core weights are 33 g and 64 g. This leads to core losses in the input transformer of **6 W**.
The core losses in the step-up transformer are 1.5 W at full power. At 40 % input power they will be neglected.

The proximity losses at full power are only 5 W, so at 40 % of the input power they can be neglected.

The losses caused by the leakage inductance of the step-up transformer, which is 1 μH are **16 W**.

The losses in the MOSFET because of reverse recovery are **15 W**.

The forward losses in the diodes are **3 W**.

The snubber losses are **16 W**.

The total expected losses are **71 W**.

Expected losses at 2 kW input power

At 2 kW input power the input current is 100 A.

The expected losses are:

- resistive losses: **113 W**
- core losses: input transformers: **6 W**
  step-up transformer **3 W**
- proximity losses in the step-up transformer: **5 W**
- losses caused by the leakage of the step-up transformer: **125 W**
- reverse recovery: **15 W**
- forward diode losses: **9 W**
- snubber losses: **16 W**

Total expected losses: **292 W**

The expected efficiency is 85 %. The transformer with build in isolation has been used to eliminate the reverse recovery losses in the diodes and the resistive losses in the MOSFETs of the altered isolation stage. One can however see that the leakage inductance, which is caused by the distance between primary and secondary winding for isolation purpose, is the biggest source of losses in the converter. These losses can be decreased by either decreasing the leakage inductance, by not integrating the isolation function or by lowering the switching frequency.
When one chooses not to integrate the transformer one can use capacitors to increase the amplification of the converter and decrease the reverse recovery losses [10].

5.2.2 Measured losses of the converter

During operation the input voltage, the output voltage and the output current have been measured using a multimeter. The four branch currents are measured with DC current probes and an oscilloscope, at the oscilloscope the currents are added and the mean value is measured. The input power is calculated by multiplying the input voltage and the input current. The output power is calculated by multiplying the output voltage and the output current. This measurement is done with different resistive loads. The maximum current that can be generated with the power supply is 40 A. The results can be found in the following table, figure 24 and figure 25:

Vin (V)	Iin (A)	Vout (V)	Iout (A)	Pin (W)	Pout (W)	Ploss (W)	Efficiency (%)
20,05	10,6	406,0	0,453	212,5	183,9	28,6	86,5
20,03	11,8	407,0	0,513	236,4	208,8	27,6	88,3
20,00	13,2	404,2	0,578	264,0	233,6	30,4	88,5
19,98	15,2	402,0	0,673	303,7	270,5	33,2	89,1
19,92	18,1	402,5	0,805	360,6	324,0	36,5	89,9
19,92	20,1	402,3	0,896	400,4	360,5	39,9	90,0
19,87	22,6	401,7	1,010	449,1	405,7	43,3	90,3
19,81	25,7	400,3	1,145	509,1	458,3	50,8	90,0
19,70	30,8	404,5	1,348	606,8	545,3	61,5	89,9
19,60	36,8	401,0	1,601	721,3	642,0	79,3	89,0

Table 1: measurement of the efficiency as a function of the input current.

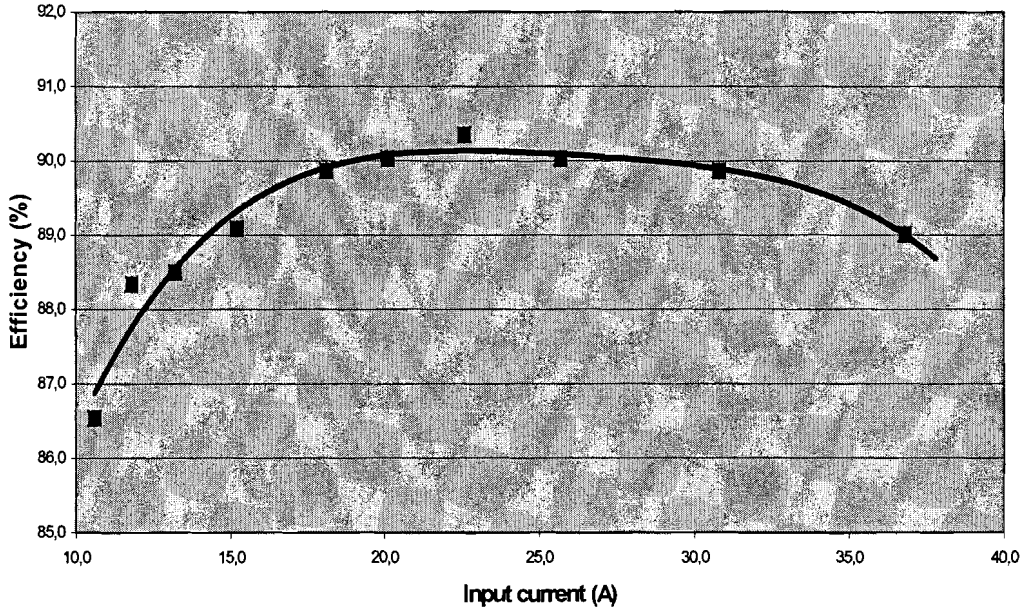

Figure 24: measured efficiency as a function of input current.

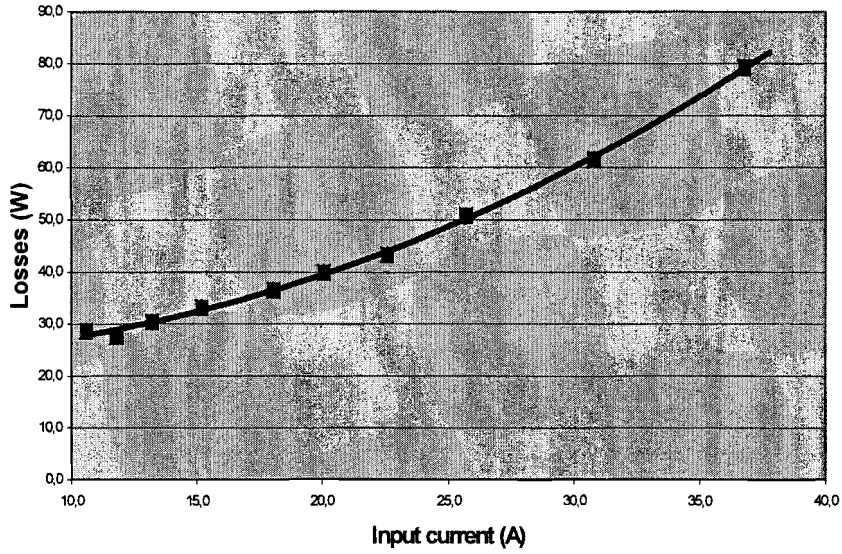

Figure 25: measured power losses as a function of input current.

5.2.3 Comparing the measured losses with the predicted losses

Measuring the losses is very hard. The input current is very high and cannot be measured using a multimeter. First, the input current was measured using a DC current probe with a large input range, which was connected to the oscilloscope using a current probe amplifier. The measurement data of this probe was compared with the data of a probe with a lower range, without an external amplifier, and had a large deviation. This deviation is probably caused by the external amplifier, which hasn't been calibrated for a long time. One decided that it would be better to measure all four input currents, add these and than measure the mean value. However, the accuracy of the current measurement is still not higher than 99 %. The accuracy of the input voltage measurement with the Fluke multimeter is 99.85 %. The error of the input power measurement is 1.15 %. At the highest measured input power of 721 W the absolute error is 8.3 W. The error in the output voltage measurement is 0.125 % and the error in the output current measurement is 0.4 %. The relative error at an output power of 642 W is 0.525%; this is an absolute error of 3.4 W. The error in the loss is 8.3 + 3.4 = 11.7 W, this is a relative error of about 15 %!

From the measurements however one can conclude that the measured and the calculated losses have large similarities. The losses are determined by constant losses, in snubbers and input transformer cores, and losses that are proportional to the square of the input current, resistive losses and losses caused by the leakage of the step-up transformer.
The measured losses however are slightly higher than the calculated losses, this can be caused by the measurement error but another possibility is that the resistances in the circuit are higher than expected because of temperature rising or insufficient effort on the lay-out of the breadboard.

In the breadboard used during this project the magnetic components have connectors that are soldered together. The solder junctions have reasonably large resistances that cause extra losses. Also reasonably thin and long wires are used to parallel the MOSFETs.
As a follow up of this project one could build a new breadboard with lower connection resistances and better connection of the MOSFETs. One should also consider the measurement of the input current, which now has a reasonably large error.

6 Conclusions and Recommendations

6.1 Conclusions

The assignment was to realise a four way interleaved boost converter for a 2 kW fuel cell system.
The power should be equally distributed over the four branches of the converter.
The converter should be able to connect a fuel cell system to the existing DC-AC converter of the EVO-2000 or the altered isolation stage that was designed during a previous traineeship.

A four way interleaved boost converter for a 2 kW fuel cell system has been realised. This converter can be used to connect the fuel cell system, with an output voltage of 20 V, to the existing EVO-2000 DC-AC converter, which has an input voltage of 400 V. The converter has an isolation function.

The transformers that couple the input currents are described in literature as components that equally distribute the input current over the converter branches. During this project was demonstrated in theory and in practice that a small difference in duty cycle between the branches, caused by component tolerances, results in large magnetizing currents through the input transformer and an unequal distribution of the input current over the branches. A control circuit has to be realised to equalize the duty cycles.

When the duty cycles are equal not only the input current is nearly ripple-less but also the branch currents are nearly ripple-less. The very small ripple that remains has four times the switching frequency of the switch in the branch. Because of this nearly ripple-less current there are no core losses in the boost inductors and the inductors can be small.

The expected losses in the converter at full power are 15 % of the input power. Most of these losses are caused by the leakage inductances of the step-up transformers. The second largest source of losses is the resistance of the magnetic components on the high current side of the step-up transformers.

6.2 Recommendations

The principal operation of the converter has been shown, but there are points for improvement of the system.

A control system should be designed which controls the duty cycles of the branches so there is no DC voltage over the magnetizing inductances of the input transformers. This control system will make sure the current is equally distributed over the branches. During this project this was done by adjusting the four duty cycles with four potentiometers, but this is very time consuming and one needs four DC current probes and four oscilloscope channels all the time.

When a new converter is build one should pay more attention to the connection of the components on the high current side of the step-up transformers. The connections used in this breadboard require a lot of soldering and this increases the resistance and therefore the losses.

To lower the losses caused by the leakage inductance of the step-up transformer there are several options. These have to be investigated to determine which is the best.
First, instead of the step-up transformers, one could use capacitors to amplify the output voltage of the boost converters. This is described in [10]. In this case, the existing isolation stage of the EVO-2000 without amplification should be used to connect the DC-DC converter to the DC-AC converter.
Second, the step-up transformers can be left out of the system and the interleaved boost converter can be connected to the altered isolation stage with amplification from a previous traineeship [5]. In this case, there will be high reverse recovery losses caused by the boost diodes.
Third, the leakage of the step-up transformers can be lowered by not integrating the isolation function and using again the existing isolation stage.
Finally, the losses caused by the leakage inductance can be decreased by lowering the switching frequency. This requires larger boost inductances for the same ripple current.

References

[1] *Hendrix, M.A.M; Rozenboom J., Duarte J.L., Michon M.M.J.A.*
Low power electronics, Power electronics below 2 kW.
Syllabus for the course Mini Power Electronics
Eindhoven University of Technology
Department Electrical Engineering
Section Electromechanics and Power Electronics

[2] *Dek, P.*
Vergelijking van de verschillende vermogensconverters.
Master of Science thesis.
March 2004
Eindhoven University of Technology
Department Electrical Engineering
Section Electromechanics and Power Electronics

[3] *Wingelaar, P.J.H.*
Characterization and modelling of a polymer electrolyte membrane fuel cell.
Master of Science thesis.
2003
Eindhoven University of Technology
Department Electrical Engineering
Section Electromechanics and Power Electronics

[4] *Hendrix, M.A.M.*
Fuel Cell Electronics.
Philips Lighting Electronics internal report LE03/10024
August 2003
Philips Business Group Lighting Electronics

[5] *Smet, B.J.M.*
A series resonant DC-DC Converter with integrated resonant inductor.
Traineeship report
September 2004
Eindhoven University of Technology
Department Electrical Engineering
Section Electromechanics and Power Electronics

[6] *Miwa, B.A.; Otten, D.M.; Schlecht, M.E.;*
High efficiency power factor correction using interleaving techniques.
Proceedings of Applied Power Electronics Conference and Exposition, 1992.
IEEE, Piscataway, NJ, USA
Pages: 557 – 568

[7] *Jang, Y.; Jovanovic, M.M.;*
New two-inductor boost converter with auxiliary transformer.
IEEE Transactions on Power Electronics.
Volume: 19, Issue: 1, Jan. 2004
IEEE, Piscataway, NJ, USA
Pages: 169 – 175

[8] *Kim, S.;*
New multiple DC-DC converter topology with a high frequency zig-zag transformer.
Proceedings of Applied Power Electronics Conference and Exposition, 2004.
Volume: 1
IEEE, Piscataway, NJ, USA
Pages: 654 – 660

[9] *Horck, F.B.M. van; Duarte, J.L.*
A treatise on Magnetics & Power Electronics.
Syllabus
January 2003
Eindhoven University of Technology
Department Electrical Engineering
Section Electromechanics and Power Electronics

[10] *Gules, R.; Pfitscher, L.L.; Franco, L.C.;*
An interleaved boost DC-DC converter with large conversion ratio.
Proceedings of International Symposium on Industrial Electronics, 2003.
Volume: 1
IEEE, Piscataway, NJ, USA
Pages: 411 – 416

Appendices

A1: Input transformer design

Transformer X:

Magnetics Common Mode Filter Inductor Design 01-05-2005

Input Parameters:

Current:	54 Amps
Inductance:	0,06 mH
Permeability:	5000
Current Density:	1000 Amps/sq.cm

Program Output Parameters:

Core Number:	ZJ-42915-TC
Header Number:	TV-H4916-4A
Filter Inductance:	58,023 uH
Cutoff Frequency:	3 Hz
Req'd Area Product:	0,220 cm4
Turns per Side:	3
Wire Size (AWG):	10
Wire Length:	2859024, cm
DC Resistance:	0,0009 Ohm
Temperature Rise:	0,1 degrees C
Est. Differential Ind.:	0,23 uH
Wound OD:	35,2 mm
Wound ID:	12,8 mm
Wound Ht:	21,4 mm

Selected Core Parameters:

Outside Diameter:	29,0 mm
Inside Diameter:	19,0 mm
Core Height:	15,2 mm
AL Value of Core:	6447 mh/1000 turns
Core Area Product:	2,1 cm4

Transformers Y and Z:

Magnetics Common Mode Filter Inductor Design 01-05-2005

Input Parameters:

Current:	27 Amps
Cutoff Frequency:	10000 Hz
Impedance:	50 Ohms
Permeability:	5000
Current Density:	1000 Amps/sq.cm

Program Output Parameters:

Core Number:	ZJ-41306-TC
Header Number:	TV-H2507-4A
Filter Inductance:	47,488 uH
Cutoff Frequency:	6 Hz
Req'd Area Product:	0,070 cm4
Turns per Side:	4
Wire Size (AWG):	13
Wire Length:	2243328, cm
DC Resistance:	0,0015 Ohm
Temperature Rise:	0,4 degrees C
Est. Differential Ind.:	0,19 uH
Wound OD:	17,3 mm
Wound ID:	3,3 mm
Wound Ht:	11,0 mm

Selected Core Parameters:

Outside Diameter:	12,7 mm
Inside Diameter:	7,9 mm
Core Height:	6,4 mm
AL Value of Core:	2958 mh/1000 turns
Core Area Product:	0,072 cm4

A2: Boost inductor design

Magnetics DC Inductor Design

Part Number:	58930-A2
Permeability:	125
Inductance Factor:	157 mH/1000 Turns
Core Area (sq cm):	0,661
Path Length (cm):	6,54
Turns:	11
Wire Size:	#13 AWG
DC Resistance:	0,003 Ohms
Header P/N:	TV-H4916-4A
Wound Core Dimensions:	1,206 x 0,621 (in inches)
Inductance (full load, µH):	10,12
Inductance (no load, µH):	19,00
Core Losses (mW):	208,9
Copper Losses (mW):	2057,5
Total Losses (mW):	2266,4
Temp. Rise (degrees C):	36,8

A3: Step-up transformer design

```
FILE:   H:\Data\Bart\Boost\Report\Measurements\stepup.txt

Mag_Tool Release 4.4

Main window title:  Mag_Tool - stepuptrafoPQ50100u.mag

SPECIFICATIONS:
===============
COMPONENT:
----------
L,Lp = 0.1 mH +- 20%
N_1  = 0.222          +- 25%
N_2  = 0.222          +- 25%
Component Name: Step_up

ARBITRARY CURRENT:
------------------
number time t/T    iL [A]      iLs_1 [A]   iLs_2 [A]
1      0           1           0           0
2      0.288       1           0           0
3      0.289       -28.25      0           6.5
4      0.5         -26.2       0           5.6
5      0.501       -1          0           0
6      0.788       -1          0           0
7      0.789       28.25       -6.5        0
8      0.999       26.2        -5.6        0
9      1           1           0           0
T = 10 us

CORE:
-----
Transformer Type:  wire wound
core_type: PQ50/50!
Rth_core = 16.4
Rth_wind = 16.4
Rth_c-w  = 0

material:  3C96
B_limit    = 300
temp_amb   = 20
temp_limit = 200

AIR GAPS:
---------
gap1: cen
position = 50
size     = 0.0207246
determine size: selected
max size = 9    50% of total
gap2: out
position = 50
size     = 0.0207246
determine size: selected
max size = 9
```

```
COIL FORMER:
------------
section left      right     bottom    top
1       0         2.5       4         28.8
2       0         9.95      0         4
3       6.7       8.9       4         28.8
4       0         9.95      28.8      32.8
5       4.5       6.7       4         28.8

WINDING LAYOUT:
---------------
section: 1
Lp   250*.04    turns = 4      in parallel =  4    connect =
options =

section: 3
Ls2  250*.04    turns = 18     in parallel =  2    connect =
options =

section: 5
Ls1  250*.04    turns = 18     in parallel =  2    connect =
options =

RESULTS:
========
DESIGN DATA:
------------
Lp    = 0.068281 [mH] at  97.7 °C
B_sat = 343 [mT] at  97.7 °C
B_max =  76.3 [mT] for Ae and   79.7 [mT] for Amin
B_min = -76.3 [mT] for Ae and  -79.7 [mT] for Amin
Al    = 6250 [nH]
u_eff = 1716
gap1  = 0.021 [mm]    gap2  = 0.021 [mm]
equivalent frequency = 192.5 [kHz]
core temperature     = 97.7 °C
winding temperature  = 97.7 °C

TOTAL LOSSES [mW]:
------------------
Winding Losses:   rms       skin   proximity    total
Lp             1732.918   188.584    603.797   2525.299
Ls1             538.212    58.776   2080.973   2677.961
Ls2             611.449    66.542   1168.360   1846.351

Specific Core Losses:          1426.337
Eddy Current Losses in Core:    999.364

Total Losses:  9475.311

EQUIVALENT CIRCUIT: not calculated
----------------------
```

B1: MOSFET data sheet

These pages contain limiting values and electrical characteristics.
For the complete data sheet download:
http://www.semiconductors.philips.com/acrobat_download/datasheets/PSMN030-150P_1.pdf

SiliconMAX

N-channel TrenchMOS™ transistor **PSMN030-150P**

FEATURES

- 'Trench' technology
- Very low on-state resistance
- Fast switching
- Low thermal resistance

SYMBOL

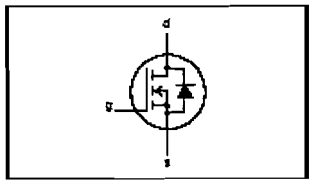

QUICK REFERENCE DATA

V_{DSS} = 150 V

I_D = 55.5 A

$R_{DS(ON)} \leq 30$ mΩ

GENERAL DESCRIPTION

SiliconMAX products use the latest Philips Trench technology to achieve the lowest possible on-state resistance in each package at each voltage rating.

Applications:-
- d.c. to d.c. converters
- switched mode power supplies

The PSMN030-150P is supplied in the SOT78 (TO220AB) conventional leaded package.

PINNING

PIN	DESCRIPTION
1	gate
2	drain
3	source
tab	drain

SOT78 (TO220AB)

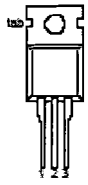

LIMITING VALUES

Limiting values in accordance with the Absolute Maximum System (IEC 134)

SYMBOL	PARAMETER	CONDITIONS	MIN.	MAX.	UNIT
V_{DSS}	Drain-source voltage	T_j = 25 °C to 175°C	-	150	V
V_{DGR}	Drain-gate voltage	T_j = 25 °C to 175°C; R_{GS} = 20 kΩ	-	150	V
V_{GS}	Gate-source voltage		-	± 20	V
I_D	Continuous drain current	T_{mb} = 25 °C	-	55.5	A
		T_{mb} = 100 °C	-	39	A
I_{DM}	Pulsed drain current	T_{mb} = 25 °C	-	222	A
P_D	Total power dissipation	T_{mb} = 25 °C	-	250	W
T_j, T_{stg}	Operating junction and storage temperature		- 55	175	°C

AVALANCHE ENERGY LIMITING VALUES

Limiting values in accordance with the Absolute Maximum System (IEC 134)

SYMBOL	PARAMETER	CONDITIONS	MIN.	MAX.	UNIT
E_{AS}	Non-repetitive avalanche energy	Unclamped inductive load, I_{AS} = 35 A; t_p = 100 µs; T_j prior to avalanche = 25°C; $V_{DD} \leq 50$ V; R_{GS} = 50 Ω; V_{GS} = 10 V;	-	300	mJ
I_{AS}	Non-repetitive avalanche current		-	35	A

THERMAL RESISTANCES

SYMBOL	PARAMETER	CONDITIONS	TYP.	MAX.	UNIT
$R_{th\ j-mb}$	Thermal resistance junction to mounting base		-	0.6	K/W
$R_{th\ j-a}$	Thermal resistance junction to ambient	SOT78 package, in free air	60	-	K/W

ELECTRICAL CHARACTERISTICS

T_j = 25°C unless otherwise specified

SYMBOL	PARAMETER	CONDITIONS	MIN.	TYP.	MAX.	UNIT
$V_{(BR)DSS}$	Drain-source breakdown voltage	V_{GS} = 0 V; I_D = 0.25 mA;	150	-	-	V
		T_j = -55°C	133	-	-	V
$V_{GS(TO)}$	Gate threshold voltage	$V_{DS} = V_{GS}$; I_D = 1 mA	2.0	3.0	4.0	V
		T_j = 175°C	1.0	-	-	V
		T_j = -55°C	-	-	6	V
$R_{DS(ON)}$	Drain-source on-state resistance	V_{GS} = 10 V; I_D = 25 A	-	24	30	mΩ
		T_j = 175°C	-	-	81	mΩ
I_{GSS}	Gate source leakage current	V_{GS} = ±10 V; V_{DS} = 0 V	-	2	100	nA
I_{DSS}	Zero gate voltage drain current	V_{DS} = 150 V; V_{GS} = 0 V;	-	0.05	10	µA
		T_j = 175°C	-	-	500	µA
$Q_{g(tot)}$	Total gate charge	I_D = 55.5 A; V_{DD} = 120 V; V_{GS} = 10 V	-	98	-	nC
Q_{gs}	Gate-source charge		-	16	-	nC
Q_{gd}	Gate-drain (Miller) charge		-	38	60	nC
$t_{d\ on}$	Turn-on delay time	V_{DD} = 75 V; R_D = 1.5 Ω;	-	18	-	ns
t_r	Turn-on rise time	V_{GS} = 10 V; R_G = 5.6 Ω	-	71	-	ns
$t_{d\ off}$	Turn-off delay time	Resistive load	-	97	-	ns
t_f	Turn-off fall time		-	76	-	ns
L_d	Internal drain inductance	Measured from tab to centre of die	-	3.5	-	nH
L_d	Internal drain inductance	Measured from drain lead to centre of die (SOT78 package only)	-	4.5	-	nH
L_s	Internal source inductance	Measured from source lead to source bond pad	-	7.5	-	nH
C_{iss}	Input capacitance	V_{GS} = 0 V; V_{DS} = 25 V; f = 1 MHz	-	3660	-	pF
C_{oss}	Output capacitance		-	470	-	pF
C_{rss}	Feedback capacitance		-	220	-	pF

REVERSE DIODE LIMITING VALUES AND CHARACTERISTICS

T_j = 25°C unless otherwise specified

SYMBOL	PARAMETER	CONDITIONS	MIN.	TYP.	MAX.	UNIT
I_S	Continuous source current (body diode)		-	-	55.5	A
I_{SM}	Pulsed source current (body diode)		-	-	222	A
V_{SD}	Diode forward voltage	I_F = 25 A; V_{GS} = 0 V	-	0.85	1.2	V
t_{rr}	Reverse recovery time	I_F = 20 A; $-dI_F/dt$ = 100 A/µs;	-	109	-	ns
Q_{rr}	Reverse recovery charge	V_{GS} = 0 V; V_R = 30 V	-	610	-	nC

B2: Diode data sheet

These pages contain limiting values and electrical characteristics.
For the complete data sheet download:
http://www.semiconductors.philips.com/acrobat_download/datasheets/BYV29X-600_1.pdf

Rectifier diodes ultrafast — BYV29X-600

FEATURES

- Low forward volt drop
- Fast switching
- Soft recovery characteristic
- High thermal cycling performance
- Low thermal resistance

SYMBOL

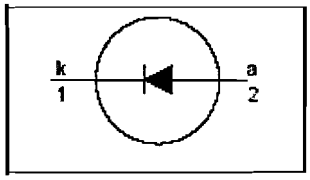

QUICK REFERENCE DATA

V_R = 600V

$V_F \leq 1.03$ V

$I_{F(peak)}$ = 7 A

$t_{rr} \leq 60$ ns

GENERAL DESCRIPTION

Ultra-fast, epitaxial rectifier diodes intended for use as output rectifiers in high frequency switched mode power supplies.

The BYV29X-600 is supplied in the conventional leaded SOD113 (SOT186a) package.

PINNING

PIN	DESCRIPTION
1	cathode
2	anode
tab	isolated

SOD113 (SOT186a)

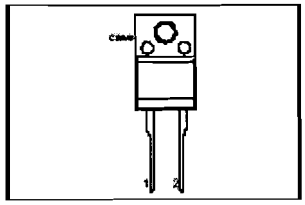

LIMITING VALUES

Limiting values in accordance with the Absolute Maximum System (IEC 134).

SYMBOL	PARAMETER	CONDITIONS	MIN.	MAX.	UNIT
V_{RRM}	Peak repetitive reverse voltage		-	600	V
V_{RWM}	Crest working reverse voltage		-	600	V
V_R	Continuous reverse voltage		-	600	V
$I_{F(AV)}$	Average forward current[1]	square wave; δ = 0.5; $T_{mb} \leq$ 100 °C	-	9	A
I_{FRM}	Repetitive peak forward current	t = 25 µs; δ = 0.5; $T_{mb} \leq$ 100 °C	-	18	A
I_{FSM}	Non-repetitive peak forward current.	t = 10 ms	-	70	A
		t = 8.3 ms	-	77	A
		sinusoidal; with reapplied $V_{RWM(max)}$			
T_{stg}	Storage temperature		-40	150	°C
T_j	Operating junction temperature		-	150	°C

THERMAL RESISTANCES

SYMBOL	PARAMETER	CONDITIONS	MIN.	TYP.	MAX.	UNIT
$R_{th\,j\text{-}hs}$	Thermal resistance junction to heat sink		-	-	5.5	K/W
$R_{th\,j\text{-}a}$	Thermal resistance junction to ambient	in free air.	-	60	-	K/W

1 Neglecting switching and reverse current losses.

ISOLATION LIMITING VALUE & CHARACTERISTIC

T_{hs} = 25 °C unless otherwise specified

SYMBOL	PARAMETER	CONDITIONS	MIN.	TYP.	MAX.	UNIT
V_{isol}	R.M.S. isolation voltage from both terminals to external heatsink	f = 50-60 Hz; sinusoidal waveform; R.H. ≤ 65% ; clean and dustfree	-		2500	V
C_{isol}	Capacitance from both terminals to external heatsink	f = 1 MHz	-	10	-	pF

ELECTRICAL CHARACTERISTICS

T_j = 25 °C unless otherwise stated

SYMBOL	PARAMETER	CONDITIONS	MIN.	TYP.	MAX.	UNIT
V_F	Forward voltage	I_F = 8 A; T_j = 150°C	-	0.90	1.03	V
		I_F = 8 A	-	1.05	1.25	V
		I_F = 20 A	-	1.30	1.45	V
I_R	Reverse current	V_R = V_{RRM}	-	2.0	50	µA
		V_R = V_{RRM}; T_j = 100 °C	-	0.1	0.35	mA
Q_s	Reverse recovery charge	I_F = 2 A to V_R ≥ 30 V; dI_F/dt = 20 A/µs	-	40	70	nC
t_{rr}	Reverse recovery time	I_F = 1 A to V_R ≥ 30 V; dI_F/dt = 100 A/µs	-	50	80	ns
I_{rrm}	Peak reverse recovery current	I_F = 10 A to V_R ≥ 30 V; dI_F/dt = 50 A/µs; T_j = 100°C	-	3.0	5.5	A
V_{fr}	Forward recovery voltage	I_F = 10 A; dI_F/dt = 10 A/µs	-	3.2	-	V

C: Data sheet of input transformer cores

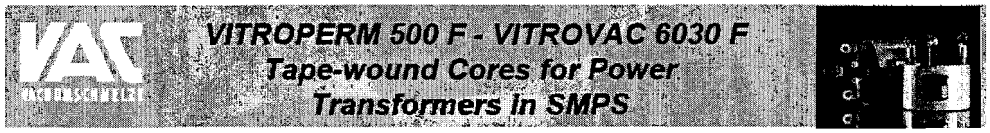

For power transformers in switched-mode power supplies, the nanocrystalline material VITROPERM 500 F and the amorphous alloy VITROVAC 6030 F offer unique advantages:

- low losses with very small temperature dependence or even negative temperature coefficients.
- high saturation flux density which is almost completely retained at high temperatures. So the SMPS - designer can choose lower operating frequencies to cost down on power semiconductors and EMI - filtering.
- sufficiently high permeability and its low dependence of flux density and temperature.
- mechanical sturdiness of the coated cores and nearly no magnetostriction of the core material enables the design of moulded components. High vibration stresses are not critical for VITROPERM.

Usually nanocrystalline VITROPERM 500 F is the best choice due to the higher saturation flux density, the improved performance and lower cost compared to amorphous VITROVAC 6030 F. But, the higher permeability of VITROPERM transformers may be problematic for the reset behaviour in high-frequency single-ended forward converter topologies. We recommend to use VITROVAC 6030 F instead. In push-pull forward converters however, high permeabilities are advantageous in most cases.

Informations on core finish:

The cores are supplied epoxy coated (Fix 350) and are suitable for direct winding. The upper limiting temperature is 120 °C.

Material data of VITROPERM 500 F/ VITROVAC 6030 F (typical values):

	VITROPERM 500 F	VITROVAC 6030 F
Saturation flux density (25 °C), B_s	1.2 T	0.8 T
Saturation flux density (100 °C), B_s	1.1 T	0.75 T
Losses (f = 20 kHz, at B_{max} = 0.2 T)	1.4 W/kg	2 W/kg
Losses (f = 100 kHz, at B_{max} = 0.2 T)	35 W/kg	40 W/kg
Curie temperature, T_c	600 °C	365 °C
Continuous upper operation temperature	120 °C	110 °C

VITROPERM 500 F and VITROVAC 6030 F - cores for transformers in SMPS, standard sizes:

core dimensions	finished dimensions (limiting values)			iron cross section and path length		core mass		A_L - value at 10 kHz typ.		winding cross section and turn length		thermal resistance	power at 20 kHz typical	part number, order code	
	O.D.	I.D.	H	A_{Fe}	l_{Fe}	m_{Fe} *	m_{Fe} **	A_L *	A_L **	A_{Cu} ***	l_{Cu}	R_{th} ****	P	VITROPERM 500 F	VITROVAC 6030 F
mm	mm	mm	mm	cm²	cm	g	g	µH	µH	cm²	cm	K/W	W	T60004-L2	T60004-E3
16x10x6	17.6	8.3	8	0.14	4.08	4.3	4.6	11	1.3	0.2	3.18	33	50	016-W373	016-F002
20x12.5x8	22	10.5	10	0.24	5.11	9	9.5	14	1.8	0.32	3.97	23	100	020-W374	020-F008
25x16x10	27	14	12	0.36	6.44	17	18	17	2.1	0.58	4.80	16	170	025-W375	025-F006
30x20x15	32.3	17.8	17.8	0.57	7.85	33	37	20	2.7	0.93	6.41	11	350	030-W376	030-F003
40x25x15	42.3	22.5	17.3	0.86	10.2	64		23		1.49	7.21	7.5	600	040-W433	-
50x40x20	52.3	37.1	22.8	0.76	14.1	79		15		4.05	9.0	4.5	1 200	050-W434	-
52x40x25	54.3	37.1	27.8	1.14	14.5	121		22		4.05	10.2	4.1	2 000	052-W827	-
55x40x25	57.5	37.1	27.8	1.43	14.9	156		28		4.05	10.5	3.9	2 500	055-W848	-
63x50x25	65.6	46.6	27.8	1.24	17.6	161		19		6.40	11.1	3.1	2 500	063-W435	-
80x63x25	83.5	59.3	27.8	1.62	22.5	267		20		10.4	12.6	2.2	4 000	080-W436	-
100x80x25	104.5	74.5	28.5	1.9	28.3	395		19		16.4	14.6	1.6	6 000	100-W342	-
130x100x25	135.5	94.5	28.5	2.85	36.1	757		22		26.3	17.2	1.1	11 000	130-W352	-
160x110x25	165	105	28.5	4.75	36.1	1480		31		32.5	19.9	0.8	16 000	160-W758	-

* VITROVAC 6030 F

** VITROPERM 500 F

*** At a winding factor of 0.5

**** Thermal resistance values are calculated based on an imaginary component using typical windings and a moulded design. No forced cooling. Values are valid for core- and windings losses and understood for a rough orientation only.

The used cores are the 030-W376 for the first input transformer and the 040-W433 for the other two input transformers.

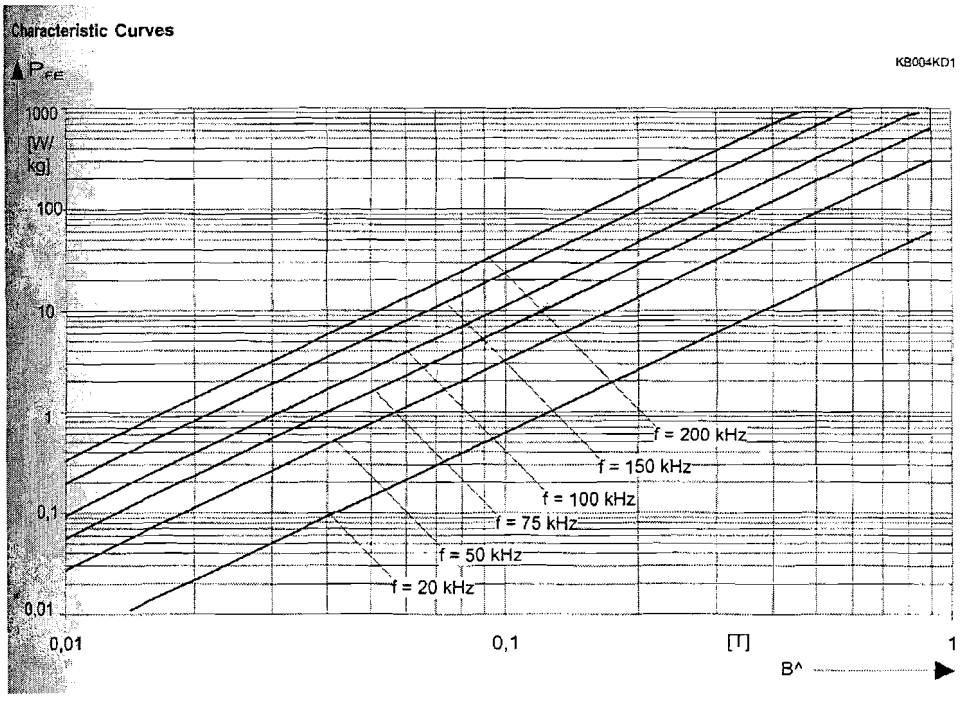
Characteristic Curves
KB004KD1
P_FE
1000
[W/
kg]
100
10
1
0,1
0,01
0,01
0,1
[T]
1
B^
f = 200 kHz
f = 150 kHz
f = 100 kHz
f = 75 kHz
f = 50 kHz
f = 20 kHz

L

Derivation of the parameters for the Steinmetz-equation x, y, Cm:
(lowest frequency range: fl_min < f < fl_max)

Input section : Specify 4 values (see Fig. 8 in the application note), B = const, T = 100°C
---------- These values should be taken at the highest possible flux density value shown in both boundary frequency curves of the actual frequency range.

f1 := 100000 1st frequency [Hz], close to the lower end of the specified frequency range (fl_min ... fl_max)

P1 := 11 specific power loss [W/kg] at B = 100 mT and for fl = 100 kHz

f2 := 200000 2nd frequency [Hz], should be close to the upper end of the specified frequency range f_min ... f_max

P2 := 40 specific power loss [W/kg] at the same value B = 100 mT and for f2 = 200 kHz

Calculation section :

$$x := \frac{\log\left(\frac{P1}{P2}\right)}{\log\left(\frac{f1}{f2}\right)}$$ eq. (35) report 1119/95

Result : x = 1.862 exponent for the frequency

Input section : Specify 4 values (see Fig. 8 in the application note), f = const, T = 100°C.

B1 := 20 1st value for the flux density [mT]

P1 := 0.4 specific power loss [W/kg] at B1 and for f = 100 kHz

B2 := 400 2nd value for the flux density [mT]

P2 := 200 specific power loss [W/kg] at B2 and for the same value f = 100 kHz

Calculation section :

$$y := \frac{\log\left(\frac{P1}{P2}\right)}{\log\left(\frac{B1}{B2}\right)}$$ eq. (35) report 1119/95

Result : y = 2.074 exponent for the flux density

M

Input section:

Specify 3 values (see Fig. 8 in the application note), T = 100°C
For each frequency range, the curves with highest power loss should be chosen as basis for the parameter Cm. So, differences between approximated values and data book values occur at curves with lower power loss and should have less impact on the power loss model.

$f := 150000$ frequency [Hz]

$B := 0.200$ flux density [T]

$poise := 100$ specific power loss [W/kg] at the selected values f and B

Calculation section:

$$Cm := \frac{poise}{f^x \cdot B^y}$$ eq. (35) report 1119/95

Result :

$Cm = 6.45 \times 10^{-7}$ factor in the Steinmetz-equation

$x = 1.862$ $y = 2.074$ $Cm = 6.45 \times 10^{-7}$

N